Theoretical Study on Bis(imino)pyridyl−Fe(II) Olefin Poly- and Oligomerization Catalysts. Dominance of Different Spin States in Propagation and β-Hydride Transfer Pathways

Dmitry V. Khoroshun, Djamaladdin G. Musaev,* Thom Vreven, and Keiji Morokuma*

Cherry L. Emerson Center for Scientific Computation and Department of Chemistry, Emory University, Atlanta, Georgia 30322

Received February 15, 2001

Mechanisms of chain propagation and β-hydride transfer (BHT) chain termination stages of poly- and oligomerization of ethylene by catalysts of general formula [2,6-(CR^1═N(($2\text{-}R^2$)-($4\text{-}R^4$)($6\text{-}R^3$)C_6H_2)$_2C_5H_3N$]$FeCl_2$ were studied theoretically. Density functional (B3LYP) and integrated molecular orbitals + molecular mechanics (IMOMM) methods were applied respectively to a model ("low steric bulk", LSB) system, [2,6-(CH═NH)$_2C_5H_3N$]$FeCH_3^+$, and one of the catalytic ("high steric bulk", HSB) systems studied experimentally, [2,6-(CMe═N(2,6-^{i}Pr$_2C_6H_3$))$_2C_5H_3N$]$FeCH_3^+$. We find that two axial ligands are required in order for the d_{z^2} orbital (with the trichelating ligand defining the equatorial *xy* plane) to be destabilized and for the singlet to be the ground state and that this is realized in BHT chain termination related species. In contrast, in the chain propagation region of potential energy surface (PES) only one axial ligand is present, where, consequently, the d_{z^2} orbital is singly occupied and the singlet becomes a low lying excited state. Our calculations on the LSB system place the lowest (singlet) BHT transition state (TS) 5.7 kcal/mol lower than the lowest (quintet and singlet) chain propagation TSs. Inclusion of both zero point energy and entropy corrections, namely, the Gibbs free energy, notably favors higher spin states, in which metal−ligand antibonding orbitals are occupied. This effect should be of general character for highly coordinated open shell transition metal complexes. On the Gibbs free energy surface of the LSB system, the lowest singlet BHT TS is only 1.0 kcal/mol lower than the lowest quintet chain propagation TS. In the HSB system, the axial positions are sterically destabilized. The main effect of increasing the steric bulk in axial position is the differentiation of the two ways of "saturating" the d_{z^2} orbital, one by destabilizing it, as in singlet species, and the other by populating it with Fe's d electron, in favor of the latter. On the PES of the HSB system, the lowest BHT TS lies 17.6 kcal/mol higher than the lowest chain propagation TS. This is in agreement with the experimentally observed suppression of BHT chain termination upon increase in steric bulk.

Downloaded by CARLI CONSORTIUM on June 29, 2009
Published on April 3, 2001 on http://pubs.acs.org | doi: 10.1021/om010126k

I. Introduction

Recently, two experimental groups independently discovered[1] a new family of highly active Fe- and Co-based olefin poly- and oligomerization catalysts. A typical precursor complex, [C_5H_3N(CR^1═N(($2\text{-}R^2$)($4\text{-}R^4$)($6\text{-}R^3$)-C_6H_2)$_2$]$FeCl_2$, is activated by methylaluminoxane (MAO) in situ (see Scheme 1). Both the length of the produced polymer chains and the structure of their end groups are highly dependent on the substituents, R^1−R^4, of the trichelating ligand. The first pronounced experimentally observed trend is an increase in the degree of polymerization with the increase in the steric bulk. Particularly, it was shown that complexes with one ortho substituent on each Ar ring ($R^2 \neq H$, $R^3 = H$; cases e−i in Scheme 1) induce oligomerization, while those bearing two ortho substituents ($R^2 \neq H$, $R^3 \neq H$; cases a−d in Scheme 1) lead to polymerization. Earlier, a similar trend was found, both experimentally[2] and theoretically,[3] for the diimine−Ni(II) and −Pd(II) catalysts.

The second experimental observation is that, for systems with one ortho substituent, the β-hydride transfer (BHT) is the dominant chain transfer mechanism, as mostly α-olefins with unsaturated end groups are produced.[1d] In contrast, for systems with two ortho substituents, end groups for produced polymers are

(1) (a) Freemantle, M. New catalysts to polymerize olefins. *Chem. Eng. News* **1998**, *Apr 13*, 11−12. (b) Britovsek, G. J. P.; Gibson V. G.; Kimberley, B. S.; Maddox, P. J.; McTavish, S. J.; Solan, G. A.; White, A. J. P., Williams, D. J. *Chem. Commun.* **1998**, *1998*, 849. (c) Small, B. L.; Brookhart, M.; Bennett, A. M. A. *J. Am. Chem. Soc.* **1998**, *120*, 4049. (d) Small, B. L.; Brookhart, M. *J. Am. Chem. Soc.* **1998**, *120*, 7143. (e) Britovsek, G. J. P.; Bruce, M.; Gibson, V. G.; Kimberley, B. S.; Maddox, P. J.; Mastroianni, S.; McTavish, S. J.; Redshaw, C.; Solan, G. A.; Stroemberg, S.; White, A. J. P.; Williams, D. J. *J. Am. Chem. Soc.* **1999**, *121*, 8728.

(2) (a) Johnson, L. K.; Killian, C. M.; Brookhart, M. S. *J. Am. Chem. Soc.* **1995**, *117*, 6414. (b) Killian, C. M.; Tempel, D. J.; Johnson, L. K.; Brookhart, M. S. *J. Am. Chem. Soc.* **1996**, *118*, 11664.

(3) (a) Deng, L.; Woo, T. K.; Cavallo, L.; Margl, P. M.; Ziegler, T. *J. Am. Chem. Soc.* **1997**, *119*, 6177. (b) Froese, R. D. J.; Musaev, D. G.; Morokuma, K. *J. Am. Chem. Soc.* **1998**, *120*, 1581. (c) Musaev, D. G.; Froese, R. D. J.; Morokuma, K. *Organometallics* **1998**, *17*, 1850.

10.1021/om010126k CCC: $20.00 © 2001 American Chemical Society
Publication on Web 04/03/2001

Scheme 1. Structures of Experimentally Studied Precursor Complexes and Corresponding Activated Catalysts; (a−d) High Steric Bulk Systems; (e−i) Low Steric Bulk Systems

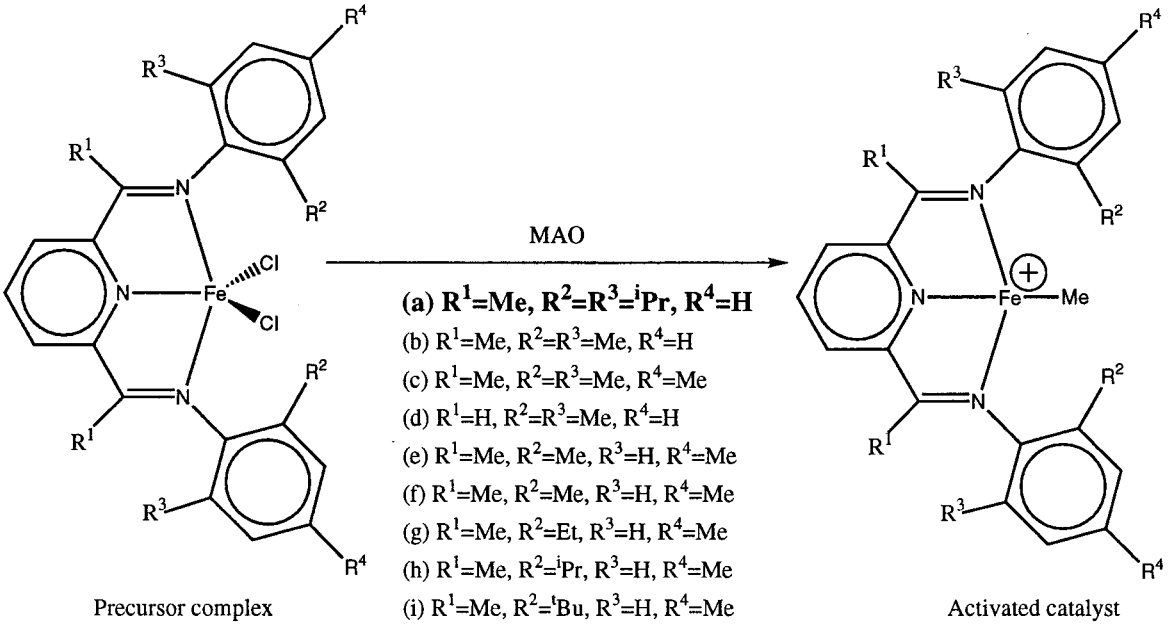

saturated, suggesting the BHT is largely suppressed, and chain termination occurs via transmetalation involving the counterion (MAO).[1b,c,e]

Summarizing the experimental data, the chemically significant result of the increase in steric bulk is twofold: (a) the increase in the degree of polymerization and (b) the change in the chain termination mechanism from BHT to transmetalation to the counterion (MAO).

Currently, no detailed mechanistic experimental results are available for the processes in question. Hence, the factors controlling the polymerization process still need comprehensive studies, which was the main inspiration for our project. Methods of computational chemistry, proven to be useful in studies of polymerization mechanisms,[4] are applied to two catalytic systems: a "model", low steric bulk (LSB) system, [2,6-(CH=NH)$_2$C$_5$H$_3$N]FeCH$_3^+$, and the "real", high steric bulk (HSB) catalyst [2,6-(CMe=N(2,6-^{i}Pr$_2$C$_6$H$_3$))$_2$C$_5$H$_3$N]-FeCH$_3^+$. The differences between the HSB and LSB systems, corresponding to increase of steric bulk, will be discussed in connection to the similar experimentally observed trends.

It is necessary for us to interpret the experimental data in such a way as to formulate a trend that may be studied computationally. Any transmetalation chain termination process (of which the importance has been suggestively mentioned by the experimentalists) cannot be studied theoretically because of the lack of information on the role of MAO and the complexity of modeling such systems theoretically. The present paper, therefore, addresses chain propagation and BHT chain termination processes. As was mentioned above, it is known from experiment that for singly ortho-substituted species BHT must be competitive with chain propagation.[1d] In the case of doubly substituted systems, chain propagation is preferred over chain termination, leading to polymer chains; chain termination, in turn, does not involve BHT, but proceeds mostly through transmetalation.[1b,c,e] Therefore, for systems with two ortho substituents on each Ar ring, BHT must be distinctively less favorable than chain propagation, while for systems with a single substituent, the two processes should be energetically comparable. The question of balance between chain propagation and BHT chain termination, and the factors that may influence this balance, is the central question of the present paper.

The goals of the present paper are (a) to study potential energy surfaces of all three possible spin states in both propagation and BHT termination regions and to rationalize the results in terms of electronic structure differences; (b) to study the effects introduced by increase in the steric bulk and to rationalize them in terms of the components of the integrated molecular orbital, MO, and molecular mechanics, MM, (IMOMM) energy; (c) to relate the results to the experimentally observed trend of suppression of the BHT chain termination mechanism upon increase of the steric bulk.

We underline the limited scope of the present paper, namely, to address a part of the experimentally observed picture, the preference of chain propagation over BHT chain termination with increase in steric bulk. The second chain termination mechanism, which involves counterion, is experimentally confirmed to be important for systems with two bulky substituents. Consequently, no conclusion on the total propagation/termination balance in such systems is possible on the basis of studies of the minor chain termination mechanism, BHT. Nevertheless, we believe that the present study provides useful insights into the mechanistic details of this complicated process, and formulation of its limited goals is justified.

Recently, two theoretical papers on the same system appeared in the literature.[5] A somewhat straightforward paper by Griffith and co-workers[5b] did not go past

(4) For instance: Yoshida, T.; Koga N.; Morokuma, K. *Organometallics* **1996**, *15*, 766. Musaev, D. G.; Morokuma, K. *Top. Catal.* **1999**, *7*, 107.

(5) (a) Deng, L.; Margl, P.; Ziegler, T. *J. Am. Chem. Soc.* **1999**, *121*, 6479. (b) Griffiths, E. A. H.; Britovsek, G. J. P.; Gibson, V. C.; Gould, I. R. *Chem. Commun.* **1999**, *1999*, 1333.

Downloaded by CARLI CONSORTIUM on June 29, 2009
Published on April 3, 2001 on http://pubs.acs.org | doi: 10.1021/om010126k

Downloaded by CARLI CONSORTIUM on June 29, 2009
Published on April 3, 2001 on http://pubs.acs.org | doi: 10.1021/om010126k

describing the polymer chain initiation step and does not overlap with the domain of our studies. Deng et al.[5a] used the same IMOMM-type methodology, but both MO and MM methods were different from ours: we use a B3LYP:MM3 combination, while Deng et al. used BP86:Amber (see below for more details). Deng and co-workers studied both chain propagation and BHT chain termination (as well as BHE chain termination) and used similar models. However, our results differ significantly and qualitatively from the results of Deng et al.; we devote a separate section of our paper to describe the differences and to speculate on the possible underlying reasons.

II. Computational Methods

To study the variation in the behavior of the system with changes in the steric hindrance, we considered the following two catalytic systems. A "model" system, [2,6-(CH=NH)$_2$C$_5$H$_3$N]-FeCH$_3^+$ + C$_2$H$_4$, is called a "low steric bulk" (LSB) system. The second, "real" system is one of the actual catalysts (case a in Scheme 1), [2,6-(CMe=N(2,6-^{i}Pr$_2$C$_6$H$_3$))$_2$C$_5$H$_3$N]FeCH$_3^+$ + C$_2$H$_4$, and is called a "high steric bulk" (HSB) system. We believe that the differences between LSB and HSB systems may be qualitatively related to the experimentally observed differences between singly and doubly ortho-substituted complexes.

An important aspect of these calculations is the spin multiplicity of the species under study. Three states (singlet, triplet, and quintet) are possible for an Fe(II) complex. In our LSB and HSB systems, three sp^2-N ligands and one alkyl ligand are present throughout the entire catalytic cycle. As will be discussed later, ethylene and the agostic bond act as two additional ligands for some structures. For certain analogous Fe(II) systems, several closely lying states with different spin multiplicity have been observed both experimentally[6] and theoretically.[7] In the present paper we attempted to study all three states.

Low Steric Bulk System. The "low steric bulk" (LSB) system, [2,6-(CH=NH)$_2$C$_5$H$_3$N]FeC$_3$H$_7^+$ + C$_2$H$_4$, was studied using the Kohn−Sham DFT method, particularly Becke's three-parameters hybrid exchange functional[8] in conjunction with Lee, Yang, and Parr's correlation functional,[9] the so-called B3LYP method. For optimization of stationary points and calculation of vibrational frequencies (including zero point energy (ZPE) correction and the entropy correction at 298.15 K and 1 atm), we used basis set I (BSI), a combination of the 3-21G basis set[10] for all atoms of the 2,6-(CH=NH)$_2$C$_5$H$_3$N ligand and the LANL2DZ (D95V[11]) basis set on the remaining atoms, including an associated nonrelativistic effective core potential for the Fe atom.[12] All calculated structures related to this "model" system will be denoted with prefix *m-* (for model system). Several benchmark studies[13] (in relation to results of high-level ab initio methods), as well as numerous applications[14] (in relation to experimentally determined parameters and trends), reveal general appropriateness of gradient-corrected density functional methods, such as B3LYP, in studies of transition metal complexes. We believe that B3LYP/BSI studies of the LBS system are sufficient to reproduce major aspects of electronic structure in the vicinity of the reaction center. As will be discussed below, we have also performed single-point calculations with a larger basis set at BSI-optimized geometries.

The results constitute our first approximation to geometries and energetics of systems of both low and high steric bulk. Moreover, the LSB system, which has no aromatic (Ar) substituents, will be used as one of the two extreme cases with respect to the degree of the steric bulk, analogous to experimentally studied systems with one ortho substituent on the Ar rings.

High Steric Bulk System. An integrated MO + MM (IMOMM[15]) method was applied to the second extreme case, a "high steric bulk" system, [2,6-(CMe=N(2,6-^{i}Pr$_2$C$_6$H$_3$))$_2$C$_5$H$_3$N]-FeC$_3$H$_7^+$ + C$_2$H$_4$, which is one of the experimentally studied systems with two ortho substituents. We use the prefix *r-* (for real system) to denote the obtained structures. In our calculations, the electronically important part of the molecule, identical to the LSB system described above, was treated at the B3LYP/BSII level. The basis set II (BSII) used for geometry optimizations was simply LANL2DZ (D95V[11]) basis set for all atoms, with the corresponding ECP and basis on Fe.[12] The remaining parts of the system (two Me and two 2,6-^{i}Pr$_2$C$_6$H$_3$ "bulky" substituents) were described by MM3 molecular

(6) (a) Nartin, L. M.; Hagen, K. S.; Hauser, A.; Martin, R. L.; Sargeson, A. M. *J. Chem. Soc., Chem. Commun.* **1988**, *1988*, 1313. (b) Diebold, A.; Hagen, K. S. *Inorg. Chem.* **1998**, *37*, 215. (c) Guetlich, P. *Coord. Chem. Rev.* **1990**, *97*, 1. (d) Guetlich, P.; Jung, J. *J. Mol. Struct.* **1995**, *347*, 21. (e) Hauser, A.; Jeftic, J.; Romstedt, H.; Hinek, R.; Spiering, H. *Coord. Chem. Rev.* **1999**, *190−192*, 471.

(7) (a) Hawkins, T. W.; Hall, M. B. *Inorg. Chem.* **1980**, *19*, 1735. (b) Kashiwagi, H.; Obara, S. *Int. J. Quantum Chem.* **1981**, *20*, 843. (c) Obara, S.; Kashiwagi, H. *J. Chem. Phys.* **1982**, *77*, 3155. (d) Rohmer, M.-M.; Dedieu, A.; Veillard, A. *Chem. Phys.* **1983**, *77*, 449. (e) Sontum, S. F.; Case, D. A.; Karplus, M. *J. Chem. Phys.* **1983**, *79*, 2881. (f) Strich, A.; Veillard, A. *Nouv. J. Chem.* **1983**, *7*, 347. (g) Newton, J. E.; Hall, M. B. *Inorg. Chem.* **1984**, *23*, 4627. (h) Rohmer, M.-M.; Strich, A.; Veillard, A. *Theor. Chim. Acta* **1984**, *65*, 219. (i) Rawling, D. C.; Gouterman, M.; Davidson, E. R.; Feller, D. *Int. J. Quantum Chem.* **1985**, *28*, 773. (j) Rawling, D. C.; Gouterman, M.; Davidson, E. R.; Feller, D. *Int. J. Quantum Chem.* **1985**, *28*, 797. (k) Rohmer, M.-M. *Chem. Phys. Lett.* **1985**, *116*, 44. (l) Saito, M.; Kashiwagi, H. *J. Chem. Phys.* **1985**, *82*, 848. (m) Sontum, S. F.; Case, D. A. *J. Am. Chem. Soc.* **1985**, *107*, 4013. (n) Edwards, W. D.; Weiner, B.; Zerner, M. C. *J. Am. Chem. Soc.* **1986**, *108*, 2196. (o) Saito, M.; Kashiwagi, H. *Int. J. Quantum Chem. Quantum Chem. Symp.* **1987**, *21*, 661. (p) Rohmer, M.-M. *Inorg. Chem.* **1989**, *28*, 4574. (q) Delley, B. In *Density Functional Methods in Chemistry*; Labanowski, J. K., Andzelm, J. W., Eds.; Springer-Verlag: New York, 1991; Chapter 7. (r) Delley, B. *Physica B* **1991**, *172*, 185. (s) Sahoo, N.; Ramani Lata, K.; Das, T. P. *Theor. Chim. Acta* **1992**, *82*, 285. (t) Matsuzawa, N.; Ata, M.; Dixon, D. A. *J. Phys. Chem.* **1995**, *99*, 7698. (u) Belazoni, P.; N., Re.; Rosi, M.; Sgamellotli, A.; Baerends, E. J.; Floriani, C. *Inorg. Chem.* **1996**, *35*, 7776. (v) Zwaans, R.; van Lenthe, J. H.; den Boer, D. H. W. *J. Mol. Struct.: THEOCHEM* **1996**, *367*, 15. (w) Lehnert, N.; Wiesler, B. E.; Tuczek, F.; Hennige, A.; Sellmann, D. *J. Am. Chem. Soc.* **1997**, *119*, 8869. (x) Rovira, C.; Kunc, K.; Hutter, J.; Ballone, P.; Parrinello, M. *J. Phys. Chem. A* **1997**, *101*, 8914. (y) Choe, Y.-K.; Hashimoto, T.; Nakano, H.; Hirao, K. *Chem. Phys. Lett.* **1998**, *295*, 380. (z) Kozlowski, P. M.; Spiro, T. G.; Bérces, A.; Zgierski, M. Z. *J. Chem. Phys. B* **1998**, *102*, 2603. (aa) Choe, Y.-K.; Nakajima, T.; Hirao, K. *J. Chem. Phys.* **1999**, *111*, 3837. (bb) Vogel, K. M.; Kozlowski, P. M.; Zgierski, M. Z.; Spiro, T. G. *J. Am. Chem. Soc.* **1999**, *121*, 9915.

(8) (a) Becke, A. D. *Phys. Rev. A* **1988**, *38*, 3098. (b) Becke, A. D. *J. Chem. Phys.* **1993**, *98*, 5648. (c) Frisch, M. J.; Trucks, G. W.; Schlegel, H. B.; Gill, P. M. W.; Johnson, B. G.; Wong, M. W.; Foresman, J. B.; Robb, M. A.; Head-Gordon, M.; Replogle, E. S.; Gomperts, R.; Andres, J. L.; Raghavachari, K.; Binkley, J. S.; Gonzalez, C.; Martin, R. L.; Fox, D. J.; Defrees, D. J.; Baker, J.; Stewart, J. J. P.; Pople, J. A. *Gaussian 92/DFT*; Gaussian Inc, Pittsburgh, PA, 1993.

(9) Lee, C.; Yang, W.; Parr, R. G. *Phys. Rev. B* **1988**, *37*, 785.

(10) J. S. Binkley, J. A. Pople, W. J. Hehre. *J. Am. Chem. Soc.* **1980**, *102*, 939.

(11) Dunning, T. H., Jr.; Hay, P. J. In *Modern Theoretical Chemistry*; Schaefer, H. F., III, Ed.; Plenum: New York, 1977; Vol. 3, pp 1−27.

(12) Hay, P. J.; Wadt, W. R. *J. Chem. Phys.* **1985**, *82*, 299.

(13) (a) Delley, B.; Wrinn, M.; Lüthi, H. P. *J. Chem. Phys.* **1994**, *100*, 5785. (b) Russo, T. V.; Martin, R. L.; Hay, P. J. *J. Chem. Phys.* **1994**, *101*, 7729. (c) Eriksson, L. A.; Petersson, L. G. M.; Siegbahn, P. E. M.; Wahlgren, U. *J. Chem. Phys.* **1995**, *102*, 872. (d) Holthausen, M. C.; Heinemann, C.; Cornehl, H. H.; Koch, W.; Schwarz, H. *J. Chem. Phys.* **1995**, *102*, 4931. (e) Holthausen, M. C.; Mohr, M.; Koch, W. *Chem. Phys. Lett.* **1995**, *240*, 245. (f) Ricca, A.; Bauschlicher, C. W., Jr. *Theor. Chim. Acta* **1995**, *92*, 123. (g) Salahub, D. R.; Chrétien, S.; Milet, A.; Proynov, E. I. Performance of Density Functionals for Transition States. In *Transition State Modeling for Catalysis*; Truhlar, D. G., Morokuma, K., Eds.; ACS Symposium Series 721; American Chemical Society: Washington, DC, 1999; pp 20−32.

(14) Davidson, E. R. *Chem. Rev.* **2000**, *100*, 351, and reviews in the same issue.

(15) (a) Maseras, F.; Morokuma, K. *J. Comput. Chem.* **1995**, *16*, 1170. (b) Matsubara, T.; Maseras, F.; Koga, N.; Morokuma, K. *J. Phys. Chem.* **1996**, *100*, 2573. (c) Matsubara, T.; Sieber, S.; Morokuma, K. *Int. J. Quantum Chem.* **1996**, *60*, 1101.

Downloaded by CARLI CONSORTIUM on June 29, 2009
Published on April 3, 2001 on http://pubs.acs.org | doi: 10.1021/om010126k

mechanics force field[16] without the electrostatic contributions. The UFF van der Waals parameters by Rappé et al. were used for the Fe atom,[17] while all other MM contributions involving the metal atom were set to zero. The fixed[15] linked bond lengths were $r(C_{sp2}-H) = 1.09$ Å, $r(N-H) = 1.03$ Å, $r(C_{sp2}-C_{sp3}) = 1.52$ Å, $r(N-C_{Ar}) = 1.38$ Å. The details of the IMOMM methodology can be found elsewhere.[15]

Several studies[3,5a,15,18] support the ability of IMOMM methods, similar to IMOMM(B3LYP/BSII:MM3) used in this paper, to properly describe steric effects. Of course, the electronic effects of the (bulky) substituents are neglected in IMOMM treatment. However, in the present case we expect the electronic effects from the substituents to be much less important than the steric effects and the IMOMM results on the actual system to be a much better approximation to the experimental data than the pure DFT calculations on the model LSB system. The IMOMM-optimized geometries are our best approximation to structures of the real catalyst (case a in Scheme 1) and related species involved in polymerization. However, we underline our intention to use the HSB system results only for conclusions based on comparison with the LSB system.

Additionally, we performed single point energy calculations for both LSB and HSB systems using large basis sets, with the aim to improve energetics and allow for a direct comparison of the results for these two systems. This basis set, BSIII, consisted of Stuttgart−Dresden ECP and the associated [8s7p6d1f]/(6s5p3d1f) basis set[19] on the Fe atom and the 6-311G(d,p) basis set[20] on the remaining atoms. The resulting B3LYP/BSIII//B3LYP/BSI and IMOMM(B3LYP/BSIII:MM3)//IMOMM(B3LYP/BSII:MM3) energies are our best approximations to the discussed species.

For the LSB system, the vibrational eigenvectors corresponding to the reaction coordinate (with imaginary frequency) of all the transition states were visually checked to confirm connectivity of transition states with the reactants and the products. No IRC calculations were performed.

The calculations were performed with Gaussian 94,[21] as well as with our own combination of the MM3(92)[22] program with Gaussian 92/DFT[8c] or Gaussian 98.[23] All triplet (**T**) and quintet (**Q**) calculations were performed with spin-unrestricted Kohn−Sham (KS) SCF. No symmetry constraints were implied during geometry optimization. For all calculations, the KS SCF density matrix change root-mean-square convergence criteria were set to 10^{-5} electron. Canonical Kohn−Sham orbitals were analyzed utilizing the Molden3.4 visualization program.[24]

Below, we organized this paper as follows. Section III contains our results, with the LSB system discussed in A. The aspects of the electronic structure of the species under study are discussed in part B, and Part C addresses the HSB system, concentrating on and rationalizing the differences relative to the LSB system. Section IV addresses the difference between our results and the results of the recently published theoretical studies on exactly the same system. In the final section, section V, we make several conclusions.

The adopted mechanisms of polymer chain propagation and β-hydride transfer (BHT) are presented in Scheme 2. The polymer chain propagation was assumed to proceed via the Cossee−Arlman[25] mechanism involving (i) coordination of the olefin to the alkyl complex (**I**), $[N_3]Fe(CH_2CH_2CH_3)^+$, to form alkyl ethylene π-complexes (**II**), and (ii) insertion of ethylene into the metal−alkyl bond via a four-center transition state (**III**) to form alkyl complex **IV**, $[N_3]Fe((CH_2CH_2)_2CH_3)^+$. In Scheme 2, we describe all these structures and the possible isomerization processes between them in greater detail.

We describe most of these structures symbolically as having octahedral configuration with the trichelating bis(imino)-pyridyl ligand defining an (approximate) equatorial (*xy*) plane. Some coordination sites of the octahedron, namely, two axial and one equatorial position, are available for the remaining ligands, such as alkyl, ethylene, agostic C−H bond, or hydride. Singlet and triplet states of compounds **I**, **II**, and **IV** are grouped into two sets of isomers based on the position of the alkyl ligand. The first group, called *axial* structures and denoted with ***ax*** following the Roman number (such as (**I-*ax***)), are species in which the alkyl ligand occupies one of the two available axial positions (along the *z* axis). The isomers of the second group, in which the alkyl ligand occupies the equatorial position, trans relative to the pyridyl's nitrogen (along the *y* axis), are called *equatorial* and are marked with ***eq*** (as in (**I-*eq***)). For the quintet state of species **I**, **II**, and **IV**, no axial/equatorial notation is introduced, since quintet species are found to be significantly displaced from the octahedral configuration.

(16) Pettersson, I.; Liljefors T. Molecular Mechanics Calculated Conformational Energies of Organic Molecules: A Comparison of Force Fields. In *Reviews in Computational Chemistry*; Lipkowitz, K. B., Boyd, D. B., Eds.; VCH: New York, 1996; Vol. 9, pp 167−189.

(17) Rappe, A. K.; Casewit, C. J.; Colwell, K. S.; Goddard, W. A., III; Skiff, W. M.; *J. Am. Chem. Soc.* **1992**, *114*, 10024.

(18) (a) Barea, G.; Maseras, F.; Jean, Y.; Lledos, A. *Inorg. Chem.* **1996**, *35*, 6401. (b) Froese, R. D. J.; Morokuma, K. *Chem. Phys. Lett.* **1996**, *263*, 393. (c) Svensson, M.; Humbel, S.; Froese, R. D. J.; Matsubara, T.; Sieber, S.; Morokuma, K. *J. Phys. Chem.* **1996**, *100*, 19357. (d) Ujaque, G.; Maseras, F.; Lledos, A. *Theor. Chim. Acta* **1996**, *94*, 67. (e) Ujaque, G.; Maseras, F.; Eisenstein, O. *Theor. Chem. Acc.* **1997**, *96*, 146. (f) Ujaque, G.; Maseras, F.; Lledos, A. *J. Org. Chem.* **1997**, *62*, 7892. (g) Wakatsuki, Y.; Koga, N.; Werner, H.; Morokuma, K. *J. Am. Chem. Soc.* **1997**, *119*, 360. (h) Barea, G.; Lledos, A.; Maseras, F.; Jean, Y. *Inorg. Chem.* **1998**, *37*, 3321. (i) Jaffart, J.; Mathieu, R.; Etienne, M.; McGrady, J. E.; Eisenstein, O.; Maseras, F. *Chem. Commun.* **1998**, *18*, 2011. (j) Maseras, F. *New J. Chem* **1998**, *22*, 327. (k) Maseras, F.; Eisenstein, O. *New J. Chem* **1998**, *22*, 5. (l) Ujaque, G.; Cooper, A. C.; Maseras, F.; Eisenstein, O.; Caulton, K. G. *J. Am. Chem. Soc.* **1998**, *120*, 361. (m) Ujaque, G.; Maseras, F.; Eisenstein, O.; Liable-Sands, L.; Rheingold, A. L.; Yao, W.; Crabtree, R. H. *New J. Chem* **1998**, *22*, 1493. (n) Woo, T. K.; Cavallo, L.; Ziegler, T. *Theor. Chem. Acc.* **1998**, *100*, 307. (o) Aiga, F.; Tada, T. *Int. J. Quantum Chem.* **1999**, *71*, 403. (p) Cooper, A. C.; Clot, E.; Huffman, J. C.; Streib, W. E.; Maseras, F.; Eisenstein, O.; Caulton, K. G. *J. Am. Chem. Soc.* **1999**, *121*, 97. (q) Dapprich, S.; Komaromi, I.; Byun, K. S.; Morokuma, K.; Frisch, M. J. *J. Mol. Struct.: THEOCHEM* **1999**, *461−462*, 1. (r) Khoroshun, D. V.; Musaev, D. G.; Morokuma, K. *Organometallics* **1999**, *18*, 5653. (s) Margl, P.; Deng, L.; Ziegler, T. *Organometallics* **1999**, *18*, 5701. (t) Maseras, F. *Top. Organomet. Chem.* **1999**, *4*, 165. (u) Shoemaker, J. R.; Burggraf, L. W.; Gordon, M. S. *J. Phys. Chem. A* **1999**, *103*, 3245. (v) Ujaque, G.; Maseras, F.; Lledos, A. *J. Am. Chem. Soc.* **1999**, *121*, 1317. (w) Woo, T. K.; Margl, P. M.; Deng, L.; Cavallo, L.; Ziegler, T. *Catal. Today* **1999**, *50*, 479. (x) Woo, T. K.; Ziegler, T. *J. Organomet. Chem.* **1999**, *591*, 204. (y) Woo, T. K.; Bloechl, P. E.; Ziegler, T. *J. Phys. Chem. A* **2000**, *104*, 121.

(19) Dolg, M.; Wedig, U.; Soll, H.; Preuss, H. *J. Chem. Phys.* **1987**, *86*, 866.

(20) Krishnan, R.; Binkley, J. S.; Seeger, R.; Pople, J. A. *J. Chem. Phys.* **1980**, *72*, 650.

(21) Frisch, M. J.; Trucks, G. W.; Schlegel, H. B.; Gill, P. M. W.; Johnson, B. G.; Robb, M. A.; Cheeseman, J. R.; Keith, T.; Petersson, G. A.; Montgomery, J. A.; Raghavachari, K.; Al-Laham, M. A.; Zakrzewski, V. G.; Ortiz, J. V.; Foresman, J. B.; Cioslowski, J.; Stefanov, B. B.; Nanayakkara, A.; Challacombe, M.; Peng, C. Y.; Ayala, P. Y.; Chen, W.; Wong, M. W.; Andres, J. L.; Replogle, E. S.; Gomperts, R.; Martin, R. L.; Fox, D. J.; Binkley, J. S.; Defrees, D. J.; Baker, J.; Stewart, J. P.; Head-Gordon, M.; Gonzalez, C.; Pople, J. A. *Gaussian 94, Revision A.1*; Gaussian Inc.: Pittsburgh, PA, 1995.

(22) (a) *MM3(92)*, Quantum Chemistry Program Exchange; Indiana University, 1992. (b) Aped, A.; Allinger, N. L. *J. Am. Chem. Soc.* **1992**, *114*, 1.

(23) Frisch, M. J.; Trucks, G. W.; Schlegel, H. B.; Scuseria, G. E.; Robb, M. A.; Cheeseman, J. R.; Zakrzewski, V. G.; Montgomery, J. A., Jr.; Stratmann, R. E.; Burant, J. C.; Dapprich, S.; Millam, J. M.; Daniels, A. D.; Kudin, K. N.; Strain, M. C.; Farkas, O.; Tomasi, J.; Barone, V.; Cossi, M.; Cammi, R.; Mennucci, B.; Pomelli, C.; Adamo, C.; Clifford, S.; Ochterski, J.; Petersson, G. A.; Ayala, P. Y.; Cui, Q.; Morokuma, K.; Malick, D. K.; Rabuck, A. D.; Raghavachari, K.; Foresman, J. B.; Cioslowski, J.; Ortiz, J. V.; Baboul, A. G.; Stefanov, B. B.; Liu, G.; Liashenko, A.; Piskorz, P.; Komaromi, I.; Gomperts, R.; Martin, R. L.; Fox, D. J.; Keith, T.; Al-Laham, M. A.; Peng, C. Y.; Nanayakkara, A.; Gonzalez, C.; Challacombe, M.; Gill, P. M. W.; Johnson, B.; Chen, W.; Wong, M. W.; Andres, J. L.; Gonzalez, C.; Head-Gordon, M.; Replogle, E. S.; Pople, J. A. *Gaussian 98, Revision A.7*; Gaussian, Inc.: Pittsburgh, PA, 1998.

(24) Schaftenaar, G.; Noordik, J. H. *J. Comput.-Aided Mol. Des.* **2000**, *14*, 123.

(25) (a) Cossee, P. *J. Catal.* **1964**, *3*, 80. (b) Arlman, E. J. *J. Catal.* **1964**, *3*, 89.

Scheme 2. Proposed Mechanism of *β*-Hydride Chain Transfer and Chain Propagation Cycle of Oligo- and Polymerization Processes for the Singlet PES[a]

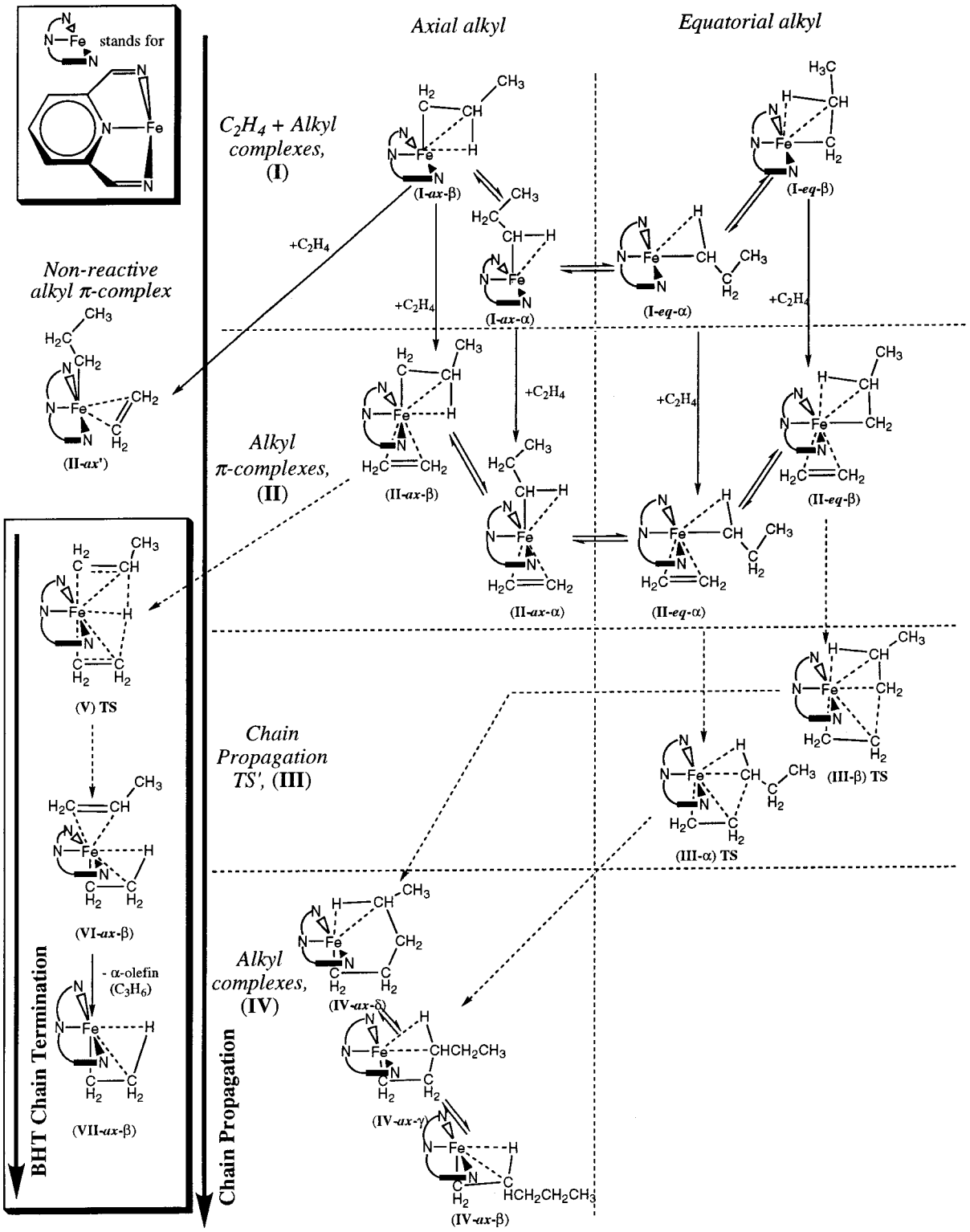

[a] Certain local minima do not exist on triplet and quintet surfaces.

Additionally, specifics of the agostic binding/alkyl ligand conformation are represented with a Greek letter following the numbers; for example, the axial isomer of complex **I** possessing a *β*-agostic bond is labeled **I-*ax*-*β***. It must be noted that our notation does not imply the presence of a strong agostic interaction in all isomers. In most cases, the only difference between the two isomers is the conformation of the polymer (propyl in our model) chain relative to the N_3Fe plane of the active part of the catalyst. Namely, the $C_\beta-C_\alpha-Fe-N_x'$ (see Scheme 3) dihedral angle is either close to ±30° (±150°) (in α-isomers) or close to ±90° (in *β*-isomers). When agostic interaction is weak, the energy difference between the two groups of isomers is relatively small.

Within a given catalytic cycle, species **I** may be regarded as reactants, with species **IV** being products. Analysis of the structures of alkyl ethylene *π*-complexes **II-*ax*** and **II-*eq***

Downloaded by CARLI CONSORTIUM on June 29, 2009
Published on April 3, 2001 on http://pubs.acs.org | doi: 10.1021/om010126k

Scheme 3. (a) Definition of the Atom Notation for the Propagation Species, Used in the Text and Supporting Information Tables S1 and S6. (b) Definition of the Atom Notation for the BHT Species, Used in the Text and Supporting Information Tables S2 and S7

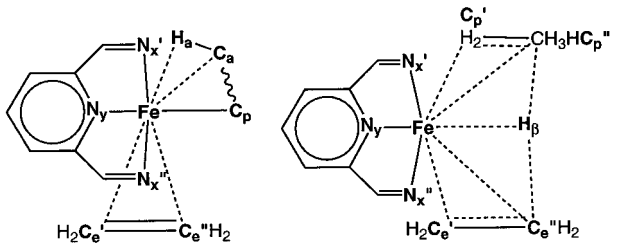

suggests that for the ethylene insertion step to occur the alkyl ligand must occupy the equatorial position, as in species **II-*eq***. The products of the insertion step, alkyl complex **IV**, formed immediately after the ethylene insertion on the singlet and triplet surfaces, are the *axial* ones. It is equivalent to saying that the catalytic cycle starts from the axial alkyl complex **I-*ax*-*β***. Consequently, singlet species **I-*ax*-*β* S** is taken as the reference for energy scale; below we use relative energies with respect to this reference. Isomer **II-*ax*** could be a precursor for the polymer chain transfer reaction involving hydrogen exchange between the alkyl (polymer) ligand and the monomer (ethylene). As seen from Scheme 2, the key point is the transition state **V**. Certain isomers of the ethyl/α-olefin (propene) complexes **VI** and the product of the α-olefin dissociation step, ethyl complexes **VII**, will also be briefly discussed.

The question of differences in energetics between chain propagation and BHT termination, the main mechanistic result of our paper, will be addressed by comparing relative energies of the corresponding transition states, namely, **III** and **V**.

III. Results and Discussion

A. Low Steric Bulk (LBS) System. The energetic parameters, calculated at the B3LYP/BSIII//B3LYP/BSI level, for the four stages of the propagation catalytic cycle (reactant alkyl complexes, ethylene alkyl *π*-complexes, insertion TS, and product alkyl complexes), as well as the BHT chain termination process of the LBS system, are summarized in Table 1. Selected regions of the potential energy profiles for the activation steps are given in Figure 1. To keep the length of the paper manageable, geometrical parameters of LBS structures, optimized at the B3LYP/BSI level, are given in Supporting Information Tables S1 (chain propagation-relevant species) and S2 (BHT-relevant species). The atomic labeling notation used in the text, as well as in Tables S1 and S2, is presented in Scheme 3.

Each of the four stages of the propagation catalytic cycle (reactant alkyl complexes, ethylene−metal−alkyl *π*-complexes, insertion TS, and product alkyl complexes), as well as BHT chain termination (Scheme 2), is discussed in a separate subsection. Except when specifically mentioned otherwise, the energetics discussed is that of B3LYP/BSIII//B3LYP/BSI without entropy or ZPE correction. The Gibbs free energy, or the effect of the entropy correction, is discussed in a separate subsection. A brief summary concludes the discussion of LBS results.

Supporting Information Table S3 contrasts energies of DZ (BSI) and TZP (BSIII) calculations. As a rule, extension of the basis set stabilizes higher spin states, especially quintet (changes in relative energies within −2 to +4 kcal/mol for singlet, −3 to +1 kcal/mol for triplet, −7 to −5 kcal/mol for quintet). Obviously, high-spin species require better basis sets (particularly, on the Fe atom) for their description.

Alkyl Complexes. Among singlet α- and *β*-agostic alkyl complexes, axial species *m*-**I-*ax*-α S** and *m*-**I-*ax*-*β* S** are 19.7 and 10.4 kcal/mol more stable than their equatorial isomers *m*-**I-*eq*-α S** and *m*-**I-*eq*-*β* S**, respectively. The strength of the *β*-agostic interaction, estimated as the energy difference between α- and *β*-isomers, is higher for equatorial species (15.6 vs 6.7 kcal/mol). These energetic parameters are in good agreement with the changes in the length of agostic bonds. In isomer *m*-**I-*ax*-*β* S**, the $C-H_a$ bond length is about 1.16 Å, compared to 1.23 Å in *m*-**I-*eq*-*β* S**; at the same time, this distance in α-isomers is only slightly larger than that for the usual C−H bond: 1.13 Å in *m*-**I-*ax*-α S** and 1.12 Å in *m*-**I-*eq*-α S**.

The triplet species *m*-**I-*ax*-*β* T**, *m*-**I-*eq*-α T**, and *m*-**I-*eq*-*β* T** are found to be 6.0, 38.6, and 23.4 kcal/mol more stable than their singlet analogues, *m*-**I-*ax*-*β* S**, *m*-**I-*eq*-α S**, and *m*-**I-*eq*-*β* S**, respectively. In contrast to the singlet, the triplet equatorial species *m*-**I-*eq*-α T** and *m*-**I-*eq*-*β* T** are more stable than the only located axial isomer (*m*-**I-*ax*-*β* T** by 6.6 and 7.0 kcal/mol, respectively. The energetic difference between equatorial α- and *β*-isomers, neither of which has agostic interaction, is negligible. We could not locate any stationary point corresponding to *m*-**I-*ax*-α T**; as soon as the weak *β*-agostic bond in *m*-**I-*ax*-*β* T** is broken, the N_y-Fe-C_p angle (see Scheme 3) starts to increase, and the system converges to an equatorial stationary point. Our attempts to locate a transition state between *m*-**I-*ax*-*β* T** and one of the *m*-**I-*eq* T** isomers also failed, indicating a small energy barrier; geometry optimizations with fixed values of the N_y-Fe-C_p angle, a coordinate that is expected to have high contribution to the true reaction coordinate, indicate less than 1 kcal/mol barrier for axial→equatorial isomerization (see Supporting Information Table S5).

On the quintet PES, we found species *m*-**I-α Q** and *m*-**I-*β* Q** to be even more stable than the triplet *m*-**I-*eq*-α T** and *m*-**I-*eq*-*β* T** by 1.6 and 3.6 kcal/mol, respectively. The value of the N_y-Fe-C_p angle in quintet species is close to 135°, and it is not possible to classify them as either axial or equatorial. We did not find any significant agostic interactions in quintet species *m*-**I Q**.

Summarizing, quintet and triplet states are the low lying states for alkyl complexes *m*-**I**, with the singlet being an excited state. Axial isomers are preferred on the singlet and destabilized on the triplet PES; no axial−equatorial classification can be applied to quintet species. Although a single-determinant method, such as Kohn−Sham DFT, is not able to rigorously address the process of conversion from axial to equatorial species on the triplet PES (see Section III.B), we roughly estimate the barrier for that isomerization to be less than 1 kcal/mol.

We found that *β*-hydride elimination (BHE), another possible chain termination mechanism that starts directly from alkyl complexes, is endothermic by at least

Downloaded by CARLI CONSORTIUM on June 29, 2009
Published on April 3, 2001 on http://pubs.acs.org | doi: 10.1021/om010126k

Table 1. Relative Energies Δ*E* and Gibbs Free Energies Δ*G* (298.15 K, 1 atm) of LSB Species *m*-I to *m*-VII at the B3LYP/BSIII//B3LYP/BSI Level Relative to *m*-I-*ax*-*β* + C_2H_4, in kcal/mol[a]

		Δ*E*			Δ*G*		
process stage	specific isomer	singlet	triplet	quintet[b]	singlet	triplet	quintet[b]
alkyl complex (*starting*	(**I-*ax*-*β***) +C_2H_4	0.0	−6.0	*b*	0.0	−9.0	*b*
point of the chain	(**I-*ax*-α**) +C_2H_4	6.7	*c*	*b*	5.3	*c*	*b*
propagation cycle)	(**I-*eq*-α**) +C_2H_4	26.0	−12.6	−14.2	23.6	−16.5	−20.0
	(**I-*eq*-*β***) +C_2H_4	10.4	−13.0	−16.6	9.4	−17.0	−22.4
alkyl ethylene *π*-complex	(**II-1′**)	−11.1 (11.1)	−14.8 (8.8)	*c*	1.2 (−1.2)	−4.7 (−4.3)	*b*
(*immediate precursors for*	(**II-*ax*-*β***)	−19.4 (19.4)	−13.5 (7.5)	*b*	−5.9 (5.9)	−4.8 (4.2)	*b*
both insertion	(**II-*ax*-α**)	−7.7 (14.4)	*c*	*b*	3.8 (1.5)	*c*	*b*
(chain propagation) and	(**II-*eq*-α**)	−7.7 (33.7)	−21.4 (8.8)	−25.7 (11.5)	4.6 (19.0)	−13.2 (−3.3)	−20.9 (0.9)
BHT (chain termination)	(**II-*eq*-*β***)	−15.1 (25.5)	−21.0 (8.0)	−26.2 (9.6)	−1.2 (10.6)	−13.1 (−3.9)	−21.7 (−0.7)
insertion (chain propagation) TS	(**III-α**)	−4.4 (3.3)	−5.6 (15.8)	−6.2 (19.5)	9.3 (4.7)	5.2 (18.4)	1.4 (19.5)
	(**III-*β***)	−6.2 (8.9)	−1.2 (19.8)	*b*	8.8 (10.0)	10.2 (23.3)	*b*
alkyl complex (*ending*	(**IV-*ax*-*δ***)	−21.5	−26.2	*b*	−6.8	−13.4	*b*
point of the chain	(**IV-*ax*-*γ***)	−20.2	−23.4	*b*	−5.4	−11.2	*b*
propagation cycle)	(**IV-*eq*-*β***)	−18.8	−27.1	*b*	−4.3	−14.7	*b*
	(**IV-*ax*-*β***)	*d*	*d*	−34.9			−26.0
BHT chain termination TS	(**V**)	−11.9 (7.5)	10.2 (23.7)	15.0 (40.7)	0.4 (6.3)	18.6 (23.4)	19.1 (40.0)
ethyl alkene *π*-complex	(**VI**)	−21.1 (19.7)	−24.8 (12.9)	−29.5 (11.5)	−7.5 (4.9)	−17.1 (0.7)	−24.6 (0.1)
ethyl complex	(**VII**) +C_3H_6	−1.4	−11.9	−18.0	−2.6	−16.4	−24.5

[a] In parentheses are C_2H_4 and C_3H_6 binding energy for species **II** and **VI**, respectively, and C_2H_4 insertion and *β*-hydride transfer activation energies for species **III** and **V**, respectively. [b] Quintet species, although not distinguished by axial/equatorial classification, are listed as equatorial. [c] Unable to locate the stationary point. [d] Locatation of the stationary point not attempted.

Downloaded by CARLI CONSORTIUM on June 29, 2009
Published on April 3, 2001 on http://pubs.acs.org | doi: 10.1021/om010126k

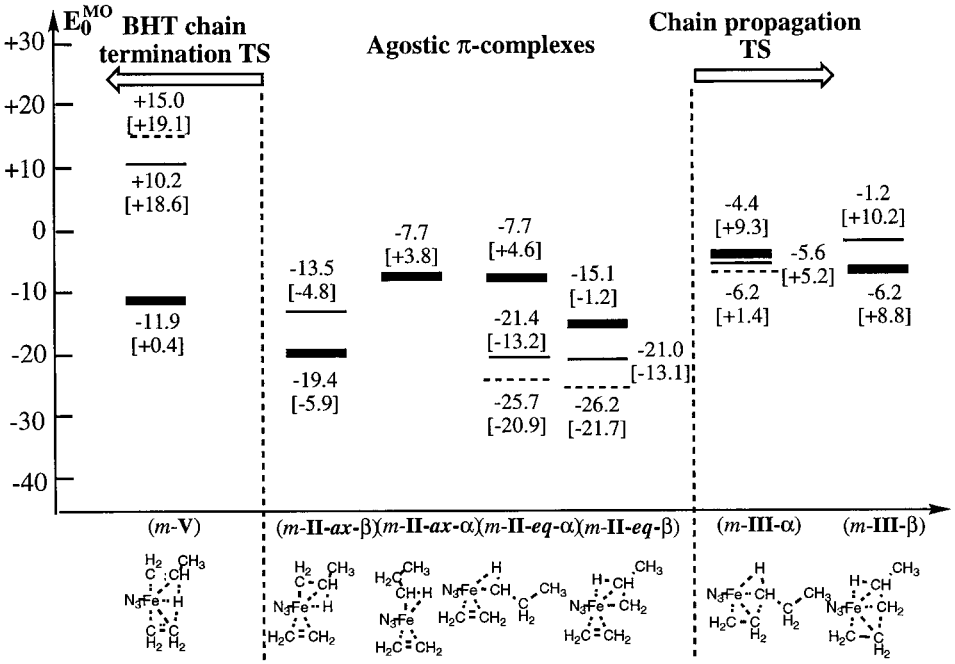

Figure 1. Competition between chain propagation and BHT chain termination mechanism in the LSB system. B3LYP/BSIII//B3LYP/BSI potential energy surfaces (in kcal/mol; in square brackets Gibbs free energy energies) for alkyl ethylene *π*-complexes *m*-**II**, propagation transition states *m*-**III**, and BHT transition states *m*-**V**. Relative to *m*-**I-*ax*-*β* S** + C_2H_4. Singlet species: thick line; triplet species: thin line; quintet species: dashed line.

10 kcal/mol for any of the three spin states. We assume that the next step for both the chain propagation and BHT chain termination processes is the barrierless coordination of the monomer, ethylene.

Monomer Capture. Upon coordination of the ethylene molecule, the singlet state structures are stabilized more than their triplet and quintet analogues. Furthermore, for the singlet state, the axial and equatorial isomers become comparable in energy (see Table 1). The ethylene binding energies are calculated to be larger for equatorial (25.5 and 33.7 kcal/mol for equatorial isomers *m*-**II-*eq*-*β* S** and *m*-**II-*eq*-α S**) than for axial (14.4 and 19.4 kcal/mol for *m*-**II-*ax*-α S** and *m*-**II-*eq*-*β* S**) species. We also located an alkyl ethylene *π*-complex, *m*-**II-*ax*′ S**, corresponding to ethylene coordination at the equatorial position, which is found to be exothermic by 11.1 kcal/mol (assuming *m*-**I-*ax*-*β* S** is the precursor). This structure is less stable than either of the *β*-alkyl *π*-complexes.

Triplet equatorial alkyl ethylene *π*-complexes *m*-**II-*eq* T** are more stable than the only located axial isomer *m*-**II-*ax*-*β* T** by about 6−8 kcal/mol. The ethylene binding energies for the triplet are somewhat smaller (8−10 kcal/mol) than for the singlet. Only *m*-**II-*ax*-*β* T** exhibits an agostic interaction of significant magnitude.

The ethylene binding energy for the quintet is 10−11 kcal/mol, comparable to that for the triplet. Interestingly, upon ethylene coordination, the N_y-Fe-C_p angle

Downloaded by CARLI CONSORTIUM on June 29, 2009
Published on April 3, 2001 on http://pubs.acs.org | doi: 10.1021/om010126k

increases in species *m*-**II-***β* **Q**, but decreases in *m*-**II-**α **Q**. Quintet species exhibit no agostic interaction.

Summarizing, the axial alkyl ethylene *π*-complexes are again preferred for the singlet (although the preference is much smaller than for alkyl complexes *m*-**I S**) and destabilized for the triplet. Most stable isomers are triplet *m*-**II-*eq* T** and quintet *m*-**II Q**, both promising precursors the for chain propagation step, and singlet *m*-**II-*ax*-*β* S**, a precursor for the BHT chain termination step. It should be emphasized that these isomers differ not only in geometrical configuration but also in the spin state. First, we report our results on chain propagation.

Ethylene Insertion. The polymer chain propagation process proceeds via a four-center insertion TS (*m*-**III**), for which we studied two conformers, *m*-**III-**α and *m*-**III-***β*. On the basis of a visual inspection of the imaginary frequency eigenvectors, these transition states are believed to connect the reactants, *m*-**II-*eq*-**α and *m*-**II-*eq*-*β***, with the corresponding products, *m*-**IV-*ax*-*γ*** and *m*-**IV-*ax*-*δ***. The singlet insertion barriers are relatively small: 3.3 and 8.9 kcal/mol. The length of the forming C_p-C_e'' bond (Scheme 3) decreases from 2.57 and 2.59 Å in the reactants *m*-**II-*eq*-α S** and *m*-**II-*eq*-*β* S** to 2.14 and 2.00 Å in the TSs *m*-**III-**α **S** and *m*-**III-*β* S**, respectively. The forming $Fe-C_e'$ bond is also shortened from 2.11 Å to 2.01 and 1.99 Å. The $C_e'-C_e''$ double bond being activated is elongated from 1.41 and 1.40 Å to 1.45 and 1.46 Å. The length of the breaking $Fe-C_p$ bond increases from 1.93 and 2.02 Å to 2.01 and 2.15 Å.

The barriers on the triplet surface are somewhat larger, 15.8 and 19.8 kcal/mol for *m*-**III-**α **T** and *m*-**III-*β* T**, respectively. The forming C_p-C_e'' bond is shortened substantially from 3.20 and 3.13 Å to 2.12 and 2.08 Å, respectively, and the length of the forming $Fe-C_e'$ bond decreases from 2.65 and 2.62 Å to 2.08 and 2.05 Å. The breaking double $C_e'-C_e''$ bond is elongated from 1.36 and 1.37 Å to 1.44 and 1.44 Å, respectively, and the breaking $Fe-C_p$ bond is stretched from 2.00 and 1.99 Å to 2.14 and 2.18 Å.

Thus, the ethylene molecule in the triplet reactants *m*-**II-*eq*-**α **T** and *m*-**II-*eq*-*β* T** is further away from the Fe center and consequently is less activated, compared to the analogous singlet species. In the singlet reactant, the forming C_p-C_e'' and $Fe-C_e'$ bonds are shorter by as much as 0.5−0.6 Å, and the breaking $C_e'-C_e''$ double bond is longer by 0.03−0.05 Å. Consequently, the structural changes required for the insertion are more significant for triplet species, and the barriers are higher.

Potentially, there is a possibility of an ethylene insertion starting from species *m*-**II-*ax′*** for both singlet and triplet. It has been found in earlier studies[3b,c,26] that analogous "perpendicular" *π*-complexes are suitable for insertion after a facile 90° rotation of the ethylene fragment. Nevertheless, we argue that such an insertion process should be mechanistically of little importance. Indeed, on the singlet surface, the product of such an insertion step would be equatorial species *m*-**IV-*eq* S**, which, analogously to species *m*-**I S**, should be highly unstable compared to axial isomers *m*-**IV-*ax* S**. Consequently, the associated insertion barrier should be prohibitively high. On the other hand, the triplet surface, already at the stage of alkyl complexes *m*-**I T**, intrinsically prefers equatorial isomers *m*-**I-*eq* T**, with the barrier for the related isomerization estimated to be small. Summarizing, singlet species *m*-**II-*ax′* S** would play a role of a "sink" unsuitable for insertion, while triplet species *m*-**II-*ax′* T** should not be formed in significant concentration due to instability of the axial coordination of the alkyl ligand.

Finally, we located only one quintet ethylene insertion TS, *m*-**III-**α **Q**, with a barrier of 19.5 kcal/mol. The breaking $C_e'-C_e''$ bond is elongated from 1.36 Å to 1.42 Å, while the forming C_p-C_e'' bond is shortened from 3.51 Å to 2.26 Å. The length of the forming $Fe-C_e'$ bond decreases from 2.68 Å to 2.15 Å, and the $Fe-C_p$ distance increases from 2.04 Å to 2.24 Å. Similar to the triplet precursor complexes *m*-**II-*eq* T**, the $C_e'-C_e''$ bond in the quintet reactant *m*-**II-**α **Q** is only slightly activated due to larger $Fe-(C_2H_4)$ separation, which leads to a relatively high insertion barrier.

Concluding, the five located insertion transition states are similar in energy, although the barriers on the singlet PES are lower due to higher energies of the precursor alkyl *π*-complexes. The singlet PES comes close in energy to triplet and quintet at the transition stage due to closer approach of ethylene to the Fe center and, consequently, a higher degree of activation of the C_2H_4 fragment in the precursor alkyl *π*-complexes *m*-**II-*eq* S**. The relative energy of the energetically lowest insertion TSs *m*-**III-**α **Q** and *m*-**III-*β* S** is −6.2 kcal/mol. The products of the insertion step are again alkyl complexes, compounds *m*-**IV**.

Alkyl Complexes. The alkyl complexes *m*-**IV** would be the same as species *m*-**I** if our model had incorporated an infinitely long alkyl (polymer) chain. In particular, *m*-**IV-*ax*-*β*** is same as *m*-**I-*ax*-*β***. While our model has a finite alkyl chain, the above-mentioned similarity still holds, and species *m*-**IV** can still be considered as the final stage of the present propagation catalytic cycle (and, correspondingly, the starting point of the next cycle).

For triplet and singlet states, we studied exclusively axial alkyl complexes, *m*-**IV-*ax*-*δ*** and *m*-**IV-*ax*-*γ***, the immediate products of the insertion, as well as the other possible axial isomer, *m*-**IV-*ax*-*β***, an analogue to *m*-**I-*ax*-*β***. As discussed for species *m*-**I**, the conversion to the equatorial isomers *m*-**IV-*eq*** should easily occur for the triplet after the axial species are formed during the ethylene insertion. In contrast, the singlet prefers axial configuration. Again, the configuration of the quintet species is neither axial nor equatorial.

The structures of the singlet species *m*-**IV-*ax* S** exhibit moderate agostic interaction (the C_a-H_a bond about 1.13−1.15 Å). The *δ*-isomer is the most stable one, with *γ*- and *β*- being 1.3 and 2.7 kcal/mol higher. The triplet species *m*-**IV-*ax* T** exhibit similarly weak agostic bonds; the *β*-isomer *m*-**IV-*ax*-*β* T** becomes the most stable one, with *δ*- and *γ*- lying 0.9 and 3.7 kcal/mol higher. The singlet−triplet separation is relatively small for *δ*- (4.7 kcal/mol) and *γ*- (3.2 kcal/mol) isomers, but is larger for the *β*-isomer (8.3 kcal/mol).

As expected from analysis of species *m*-**I**, the quintet alkyl complex *m*-**IV-*β* Q** is much more stable than either singlet or triplet axial complexes *m*-**IV-*ax***. No significant agostic interaction is found in *m*-**IV-*β* Q**.

Concluding, singlet and triplet states are close in energy for axial alkyl complexes *m*-**IV-*ax***, with the

(26) Koga, N.; Morokuma, K. *Chem. Rev.* **1991**, *91*, 823.

Downloaded by CARLI CONSORTIUM on June 29, 2009
Published on April 3, 2001 on http://pubs.acs.org | doi: 10.1021/om010126k

triplet being slightly lower, while the quintet is much lower than the other two spin states. On the basis of analogy with alkyl complexes **I**, we expect equatorial triplet species *m*-**IV-*eq* T** to be comparable in energy to the quintet minimum; equatorial singlet species must be significantly higher in energy.

Summary: Chain Propagation Cycle. The polymer chain propagation process starts from the reactant alkyl complex *m*-**I**, which is a product of the previous propagation cycle that finishes at axial species, such as *m*-**I-*ax*-β** for triplet and singlet spin states and *m*-**I-**α **Q** or *m*-**I-**β **Q** for the quintet state. However, for triplet and singlet states, in order for polymer chain propagation to occur, a conversion of these axial species into their equatorial isomers, *m*-**I-*eq***, should take place. The axial → equatorial isomerization occurs easily for the triplet, for which equatorial isomers *m*-**I-*eq* T** are more (by 6−7 kcal/mol) stable than the axial one. However, for singlet species the axial *m*-**I-*ax*-β S** isomer is the lowest among all singlet alkyl complexes and conversion to equatorial isomers is energetically very unfavorable, indicating that the starting point of the polymer chain propagation process could be either triplet *m*-**I T** or quintet *m*-**I Q** alkyl complexes. Singlet alkyl complexes *m*-**I S** are unlikely to lead to polymer chain propagation because of the high barrier for the axial → equatorial isomerization process.

Nevertheless, should singlet species *m*-**I-*ax*-β S** be formed and survive until the next monomer capture, it forms the very stable alkyl π-complex *m*-**II-*ax*-β S**. Triplet (equatorial) alkyl complexes form comparably stable equatorial species *m*-**II-*eq* T**. However, the most stable alkyl π-complexes are the quintet ones, *m*-**II Q**. Interestingly, the Gibbs free energy (which includes ZPE and entropy contribution), as shown in Table 1, favors higher spin states, triplet and especially quintet (see below for our explanation).

The relative energies of the calculated ethylene insertion transition states are comparable for all three spin states. While the β-agostic structure of the propyl (or poly- or oligomer) chain favors the singlet transition state over triplet, all three TSs of α-agostic configurations are close in energy. The energetically most favorable propagation transition states are *m*-**III-**β **S** and *m*-**III-**α **Q**, both lying at −6.2 kcal/mol relative energy. Again, the Gibbs free energy correction favors the higher spin species: *m*-**III-**α **Q** becomes +1.4 kcal/mol, and *m*-**III-**β **S** is shifted up to +8.8 kcal/mol.

BHT Chain Termination. The precursor for the chain termination process for both singlet and triplet is species *m*-**II-*ax*-β**. However, the conformation of the propyl chain in species *m*-**II-**α **Q** is more favorable for BHT than that in *m*-**II-**β **Q**.

The most stable singlet alkyl π-complex, axial *m*-**II-*ax*-β S**, is a suitable precursor for the β-hydride chain transfer process leading to chain termination. The corresponding transition state, *m*-**V S**, is the lowest in energy among all three spin states (−11.9 kcal/mol, the barrier of 7.5 kcal/mol). The breaking $C_p''-H_\beta$ bond is elongated from 1.17 Å to 1.60 Å, while the forming $C_e''-H_\beta$ bond is shortened from 2.37 Å to 1.61 Å (see Table S2). A strong interaction of the transferred hydride center with Fe exists in *m*-**V S**; the length of $Fe-H_\beta$ bond is decreased from 1.82 Å to 1.59 Å. The $C_e'-C_e''$ distance increases from 1.39 Å to 1.43 Å; correspondingly, the $C_p'-C_p''$ distance decreases from 1.51 Å to the same 1.43 Å. The forming $Fe-C_e'$ bond is shortened from 2.27 Å to 2.10 Å; the breaking $Fe-C_p'$ bond is stretched from 2.00 Å to 2.09 Å.

The triplet TS *m*-**V T** is energetically significantly higher (relative energy 10.2 kcal/mol, barrier of 23.7 kcal/mol). Both $C_e''-H_\beta$ and $C_p''-H_\beta$ distances are smaller than in the singlet TS, 1.57 and 1.54 Å, while the $Fe-H_\beta$ bond is significantly larger, 1.71 Å (Table S2). Also larger (compared to *m*-**V S**) are the $Fe-C_e'$ and $Fe-C_p'$ bonds: 2.14 and 2.12 Å.

The quintet TS *m*-**V Q** is energetically even higher (relative energy 15.0 kcal/mol). The $C_e''-H_\beta$ and $C_p''-H_\beta$ bonds are shortened further to 1.45 and 1.51 Å, while the $Fe-H_\beta$ distance is increased to 1.94 Å. The $Fe-C_e'$ and $Fe-C_p'$ distances are 2.22 and 2.14 Å, with the N_y-Fe-C_e' and N_y-Fe-C_p' angles being 102.3° and 117.3°. The quintet TS is more asymmetric than triplet and singlet ones (it is an early TS for the process of H_β transfer from ethyl to propyl). As expected, the Fe's involvement in the process (interaction of the H_β center with the $d_{x^2-y^2}$ orbital and of the two carbon atoms with the d_{z^2} orbital) favors lower spin states.

The products of BHT and subsequent α-olefin elimination, *m*-**VI** and *m*-**VII**, respectively, are very similar to *m*-**I** and *m*-**II** for singlet and quintet states. We were not able to locate a local minimum corresponding to *m*-**VI-*ax*-β T**. The trans influence of the propene ligand is larger than that of ethylene, which leads to destabilization of the ethyl ligand (see section III.B). We suggest that the direct product of the BHT process on the triplet surface is *m*-**VI-*eq*-α T**.

Summarizing, the BHT chain transfer process takes place exclusively on the singlet PES, with a relatively small barrier. Both triplet and quintet BHT transition states are prohibitively high in energy.

The Effect of Entropy: Gibbs Free Energy. It should be remembered that all discussed values of energy are relative to species *m*-**I-*ax*-β S** + C_2H_4 and are without zero point energy and entropy correction. Here we discuss the energetics in terms of the Gibbs free energy. We also distinguish the difference between the Gibbs free energy and the relative energy (discussed above), called the Gibbs energy correction, and separate it into the zero-point and entry contribution. The absolute values of both Gibbs free energy and ZPE corrections are given in Supporting Information Table S4.

To discuss Gibbs free energies, we distinguish two groups of points on the PES: those that consist of two units (bimolecular species, *m*-**I** + C_2H_4 and *m*-**VII** + C_3H_6) and those of a single unit (unimolecular species, *m*-**II** through *m*-**VI**). The difference in relative energies, introduced by the Gibbs free energy correction (at 298.15 K, 1 atm), within the first group (bimolecular species) comes mostly from internal degrees of freedom. The difference within the second (unimolecular species) group additionally includes intermolecular contribution (contribution from these degrees of freedom that are translational and rotational on infinite separation of the two units, but become vibrations in unimolecular species). Therefore, one would expect the unimolecular species to be entropically destabilized more than bimolecular species.

Downloaded by CARLI CONSORTIUM on June 29, 2009
Published on April 3, 2001 on http://pubs.acs.org | doi: 10.1021/om010126k

The calculated difference between the Gibbs free energy and potential energy for singlet unimolecular species ranges within 12−15 kcal/mol, and for singlet bimolecular species within −2 and 0 kcal/mol. The average change when going from relative energy to relative Gibbs free energy (relative Gibbs free energy correction) is 13.5 kcal/mol for the 12 unimolecular species and −1.2 kcal/mol for five bimolecular species. At the same time, the average relative ZPE correction is +2.4 kcal/mol for unimolecular and −0.5 kcal/mol for bimolecular species.

For triplet species, the changes introduced by entropic correction are −4 to −2 kcal/mol and 8−13 kcal/mol for bi- and unimolecular species, respectively. The average relative Gibbs free energy correction is +10.2 kcal/mol for 11 unimolecular triplet species and −3.7 kcal/mol for four bimolecular species. The average relative ZPE correction is +0.9 kcal/mol for unimolecular and −1.3 kcal/mol for bimolecular species. Both average relative corrections decrease for both groups of triplet species compared to the singlet. The decrease in Gibbs free energy correction is larger than in the ZPE correction, which means that the entropy correction also decreases. The decrease definitely comes from internal degrees of freedom of Fe-containing species. We explain this decrease by shallower (lower frequency) vibrations in triplet species for those modes influenced by the Fe d-block occupation (such as Fe-ligand, agostic-related, Fe-coordinated double C−C bonds; see section IIIB for discussion of the electronic structure rationalizations). Obviously, the result is a decrease in both ZPE (smaller vibrational frequencies) and entropy (larger number of populated excited vibrational states) corrections for the triplet relative to those for the singlet.

The same arguments may be used to explain even further decrease in the Gibbs free energy correction in quintet species, −7 to −5 and 4−9 kcal/mol for bi- and unimolecular species, respectively. The average relative Gibbs free energy correction is +5.8 kcal/mol for six mono- and −6.1 kcal/mol for three bimolecular species. The average relative ZPE correction is −1.0 kcal/mol for mono- and −1.9 kcal/mol for bimolecular species.

Effectively, inclusion of ZPE and entropy corrections stabilizes higher spin states (triplet and particularly quintet) compared to the lower spin state (singlet). For example, insertion transition states *m*-**III-**α **Q** and *m*-**III-***β* **S** are of similar potential energy (−6.2 kcal/mol); inclusion of the entropy correction significantly stabilizes the quintet TS (+1.4 kcal/mol in relative Gibbs free energy) relative to the TS on the singlet PES (+8.8 kcal/mol). This observation is consistent with the reported[7bb] systematic decrease of several lowest vibrational frequencies of Fe(II) porphyrins with the increase of total spin.

Summary: "Low Steric Bulk" System. Both the BHT chain termination process and propagation catalytic cycle on the singlet surface start at axial alkyl ethylene *π*-complexes, such as *m*-**II-*ax*-*β* S**. The axial → equatorial rearrangement barrier (relative to *m*-**II-*ax*-*β* S**) on the singlet PES is substantial (more than 11.7 kcal/mol) and larger than the BHT barrier of 7.5 kcal/mol, which means BHT chain termination is the lowest pathway on the singlet surface. The axial → equatorial transformation opens two propagation pathways through transition states *m*-**III-**α **S** and *m*-**III-***β* **S**, with immediate barriers of 3.3 and 8.9 kcal/mol, correspondingly. Assuming rapid interconversion between axial and equatorial *π*-complexes, one may apply the Curtin−Hammett principle[27] in order to compare the rates of chain propagation and BHT chain termination. The BHT TS *m*-**V S** is lower than the two propagation transition states by 7.5 and 5.7 kcal/mol, correspondingly. Therefore, even if the axial → equatorial isomerization takes place rapidly, the BHT pathway still remains the preferable pathway on the singlet PES.

The two chain propagation barriers on the triplet PES (15.8 and 19.8 kcal/mol), although larger than those for the singlet PES, are lower than the triplet BHT barrier (at least 23.7 kcal/mol). The two triplet chain propagation transition states are lower than the BHT TS by 15.8 and 11.4 kcal/mol. The quintet PES is quite similar to the triplet PES. The propagation barrier for the only located TS *m*-**III-**α **Q** is 19.5 kcal/mol; the BHT barrier is at least 40.7 kcal/mol. The chain propagation TS lies 21.2 kcal/mol lower than the BHT chain termination TS.

The triplet and quintet surfaces lie close in energy, with the quintet being a little lower. Both states are well suited for the catalytic chain propagation cycle. Since the Gibbs free energy correction stabilizes the quintet species relative to both the triplet and singlet, we suggest that chain propagation in low steric bulk species takes place on the quintet PES. In contrast, the BHT chain termination (which, according to experimental results, is the dominant chain transfer mechanism for low steric bulk systems) may realistically take place only on the singlet PES. Therefore, the rate of the intersystem crossing (change of spin) processes for different species is a crucial parameter of the main mechanistic question of the present paper, the competition between chain propagation and BHT chain termination. We are currently unable to rigorously address this issue. As a zero approximation, we again suggest applying the so-called Curtin−Hammett principle, in this case to the entire array of alkyl *π*-complexes *m*-**II**. Namely, assuming that the intersystem crossing processes, as well as conversion between all the isomers of alkyl *π*-complexes, are faster than both chain propagation and BHT chain termination, it is possible to assess the relative rate of the latter two processes by comparing relative energies of the corresponding transition states. Figure 1 illustrates this approach. The only important BHT chain transfer TS, *m*-**V S**, is 5.7 kcal/mol lower than the lowest chain propagation TSs, *m*-**III-**α **Q** and *m*-**III-***β* **S**; inclusion of entropy correction decreases the difference between *m*-**V S** and *m*-**III-**α **Q** to 1.0 kcal/mol. Of course, the assumption of fast intersystem crossing needs to be justified, and future studies on the subject, both theoretical and experimental, are required.

Concluding, in the case of low (absent) steric bulk, the relative energy of the BHT chain termination transition state on the singlet state is closely comparable with the relative energies of the chain propagation process on all spin states. This correlates with the experimentally observed production of α-olefins by analogous systems with single ortho substituent on the Ar rings (systems with low steric bulk).

(27) Seeman, J. I. *Chem. Rev.* **1983**, *83*, 83.

Downloaded by CARLI CONSORTIUM on June 29, 2009
Published on April 3, 2001 on http://pubs.acs.org | doi: 10.1021/om010126k

B. Low Steric Bulk System: Electronic Effects. Some of the results described in section III.A may be rationalized in terms of electronic structure of the species under study, in particular, involving the occupation patterns of the Fe d orbitals and the concept of trans influence. Our systems are positively charged d^6 complexes of Fe(II). In all of the closed shell singlet species, the occupation pattern is $(d_{xz})^2(d_{yz})^2(d_{xy})^2$; in other words, all three "d_π" orbitals are occupied, while the two "d_σ" orbitals (d_{z^2} and $d_{x^2-y^2}$) are vacant.[28] The relative stability of equatorial and axial isomers on the singlet PES is determined predominantly by the strong trans influence of alkyl and pyridyl ligands, a combination that strongly disfavors equatorial configuration. The agostic binding, however, is stronger in equatorial species, in which no ligands other than agostic C−H bond occupy the *z* axis; as a result, the electron-accepting d_{z^2} orbital lies low in energy. On the other hand, the $d_{x^2-y^2}$ orbital is always destabilized by three ligating nitrogens, and donation of agostic electron density to this orbital in axial species is less favorable.

In our unrestricted Kohn−Sham calculations, quintet and especially triplet wave functions are contaminated (poorly represented by a single determinant). The expectation value of S^2 in certain triplet species approaches 3 (pure spin single determinant value is 2). Consequently, the orbital analysis becomes less meaningful, since several pure spin determinants (occupation patterns) are superimposed. Nevertheless, reasonable rationalizations may still be suggested.

The dominant type of occupation pattern in triplet species is $(d_{xz}d_{yz}d_{xy})^5(d_{z^2})^1$, with a hole in the "$d_\pi$" three-orbital block and a single electron in the more stable of the two "d_σ" orbitals, usually d_{z^2}. Exceptions are species *m*-**II-*ax*-β T**, *m*-**V T**, and *m*-**II-*eq*-α T**, which have two ligands on the *z* axis and for which configurations $(d_{xz})^2(d_{yz})^2(d_{xy})^1$ and $(d_{xz})^2(d_{yz})^1(d_{xy})^2$ mix in the "d_π" block and $(d_{x^2-y^2})^1(d_{z^2})^0$ and $(d_{x^2-y^2})^0(d_{z^2})^1$ mix in the "d_σ" block. For all other triplet species, in which the d_{z^2} orbital is always singly occupied, the position of the single hole in the block of three "d_π" orbitals is of interest. We find that axial species (in which the strong alkyl ligand occupies a position along the *z* axis) may be approximately described as having a $(d_{xz})^1(d_{yz})^2(d_{xy})^2(d_{z^2})^1$ configuration. The d_{xz} orbital is the least stable "d_π" orbital due to the influence of the two imino nitrogens and the alkyl ligand. On the other hand, in the equatorial species (in which all four ligands lie in the *xy* plane) the d_{xy} orbital is the least stable among the three "d_π" orbitals, and therefore the $(d_{xz})^2(d_{yz})^2(d_{xy})^1(d_{z^2})^1$ occupation pattern is realized.

The fact that d_{z^2} is singly occupied in most triplet species is associated with a strong preference for equatorial species, which lack unfavorable direct interaction of the alkyl ligand orbital with d_{z^2} on Fe. Nevertheless, the trans influence of the pyridyl nitrogen ligand, which destabilizes the equatorial position, is definitely still present. The combination of the two factors results in a moderate preference of equatorial species on the triplet surface.

The occupation of the "d_σ" block ($(d_{z^2})^1(d_{x^2-y^2})^0$) is preserved during the process of axial → equatorial isomerization on the triplet surface. However, orbitals within the "d_π" block are highly mixed, and the situation is less clear. As the alkyl ligand moves from the *y* (N_y-Fe−C_p angle of 90°) to the *z* (180°) axis during that process, the "d_π" hole shifts twice; the occupation of the "d_π" block changes from $(d_{xz})^1(d_{yz})^2(d_{xy})^2$ (stable at around 120°) to $(d_{xz})^2(d_{yz})^1(d_{xy})^2$ (stable at around 135°) to $(d_{xz})^2(d_{yz})^2(d_{xy})^1$ (stable past 150°). A single-determinant Kohn−Sham formulation of the density functional theory is unable to rigorously address the question of transition state(s) on the adiabatic electronic ground state (alternatively, the question of intersection between diabatic states) associated with such a process. Since "jumps" are observed in the energy of the system (see Table S5), we may suggest that the nature of the highest point along the isomerization coordinate is better described as conical intersection between two diabatic states rather than a transition state on an adiabatic state. The transition from $(d_{xz})^1(d_{yz})^2(d_{xy})^2$ to $(d_{xz})^2(d_{yz})^1(d_{xy})^2$ state is a "jump" on the α-configuration PES, while the subsequent transition to the $(d_{xz})^2(d_{yz})^2(d_{xy})^1$ state is much smoother; for the β-configuration, the situation is reversed (smooth first transition and a "jump" during the second one). Associated with the change in the electronic state may be a rearrangement of the trichelating bis(imino)pyridyl ligand, which would change the reaction coordinate in the region of such a jump. Consequently, no rigorous estimate may be given for the effective barrier of axial → equatorial isomerization.

On the other hand, for the chain propagation step, the shift of the hole within the "d_π" block (occupation changes from $(d_{xz})^2(d_{yz})^2(d_{xy})^1$ to $(d_{xz})^1(d_{yz})^2(d_{xy})^2$) is smooth during the entire process. The hole never populates the d_{yz} orbital, and we observe that the hole-containing orbital is gradually rotated about the *x* axis, from d_{xy} (in the reactant, *m*-**II-*eq* T**) to d_{xz} (in the product, *m*-**IV-*ax* T**). The singly occupied "d_π" orbital in the transition state is a mix of the two. Therefore, the highest energy point can be determined as a TS.

The situation with the BHT process is less clear, since both the electron in the "d_σ" and the hole in the "d_π" block shift twice (reversibly) during the course of the reaction. Nevertheless, we were able to locate a rigorous transition state. During the BHT process, the occupation changes approximately from $(d_{xz})^2(d_{yz})^2(d_{xy})^1(d_{x^2-y^2})^1$ to $(d_{xz})^2(d_{yz})^2(d_{xy})^1(d_{z^2})^1$; the transition state is located on the latter electronic state. After the system passes this transition state, the occupation changes back to $(d_{xz})^2(d_{yz})^2(d_{xy})^1(d_{x^2-y^2})^1$; several possible conical intersections are all lower in energy than the located transition state *m*-**V T**. In contrast, the axial → equatorial isomerization discussed above is mostly downhill all the way, with conical intersections being local highest energy points, and no rigorous transition state was located with the present implementation of DFT.

The high lability of the axial alkyl ligand in the presence of a singly occupied d_{z^2} orbital is responsible for the fact that the species *m*-**VI-*ax*-β T** does not exist as a local minimum, while a (shallow) minimum corresponding to *m*-**II-*ax*-β T** was located. A slight increase in the trans influence of the alkene ligand (from ethene to propene) must be sufficient for destabilization of the corresponding region of the triplet PES. Partial occupation of the d_{z^2} orbital enhances the trans effect, desta-

(28) The orbitals which are of σ character with respect to at least one of the ligands, namely, d_{z^2} and $d_{x^2-y^2}$, are referred to as d_σ, while the remaining three d_{xz}, d_{yz}, and d_{xy} orbitals are denoted d_π.

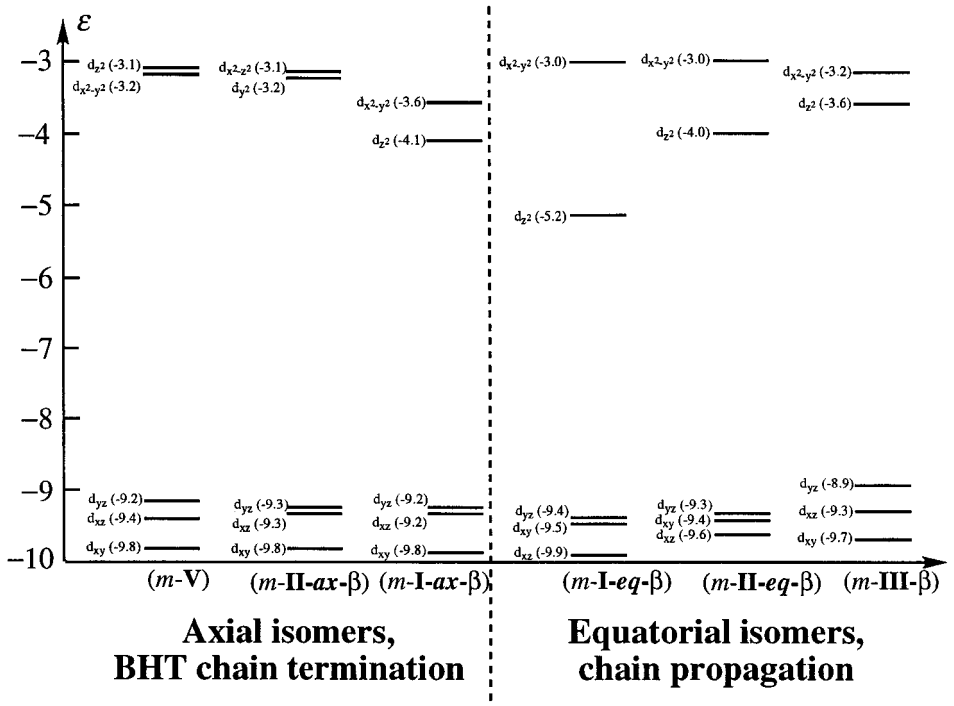

Figure 2. Kohn−Sham B3LYP/BSI canonical orbitals energies (in electronvolts) of selected singlet species.

Downloaded by CARLI CONSORTIUM on June 29, 2009
Published on April 3, 2001 on http://pubs.acs.org | doi: 10.1021/om010126k

bilizing the alkyl carbon−Fe interaction more than the stabilization due to the (already weak in the triplet species) β-agostic interaction.

The observed weakness of agostic interaction in the triplet species compared to singlet analogues may be explained in terms of the orbital energies. In the singlet species, vacant $d_{x^2-y^2}$ and especially d_{z^2} orbitals are lower in energy than the only vacant (mostly $d_{x^2-y^2}$) orbital in case of triplet species. In a sense, there is a need for an additional ligand in the singlet species, and the agostic interaction becomes a necessity.

A very approximate occupation pattern of quintet species is a mix of $(d_{xz})^2(d_{yz})^1(d_{xy})^1(d_{z^2})^1(d_{x^2-y^2})^1$ and $(d_{xz})^1(d_{yz})^1(d_{xy})^2(d_{z^2})^1(d_{x^2-y^2})^1$ configurations. Both axial positions, as well as the equatorial one, are destabilized by singly occupied d_{z^2} and $d_{x^2-y^2}$ orbitals, respectively. Consequently, the alkyl ligand occupies a position in the *yz* plane between the *y* and *z* axes (N_y−Fe−C_p angle 125−145°), destabilizing the d_{yz} orbital and making it unsuitable for occupation by the only β-spin electron. The remaining two orbitals of the "d_π" block share the only β-electron. The quintet PES, with its lack of axial/equatorial distinction, is ideal for propagation. At the same time, the quintet is the least suited spin state for BHT chain termination, since both d_{z^2} (interacting in *m*-**V Q** with the carbon atoms of partially alkyl character) and $d_{x^2-y^2}$ (interacting with the hydride) orbitals are singly occupied.

Figure 2 illustrates the Kohn−Sham orbital energies of some of the species under study. Since the d_{z^2} orbital is much more stable in the equatorial/propagation region of the PES, equatorial triplet species are more stable than axial/BHT-relevant species, in which no low lying "d_σ" orbital exists. In the case of species *m*-**II-*ax*-β S**, the "quantization axis" is *y* instead of *z*, so that the virtual "d_σ" block consists of d_{y^2} and $d_{x^2-z^2}$ orbitals. Species *m*-**V S**, in which the ligand environment is closest to that of six ligands, belongs to the region of the PES in which the singlet is the ground state. Decrease in the strength of the ligand field and stabilization of d_{z^2} orbitals (via weakening of one of the Fe−C interactions and change of the alkyl ligand position from axial to equatorial) favor higher spin states. Therefore, in the propagation region of the PES, the quintet and triplet are lower in energy than the singlet. It must be remembered that the orbitals shown in Figure 2 are those of the singlet species at the singlet optimized geometries. As follows from Tables S1 and S2, geometrical parameters (most relevantly, Fe−N distances and N−Fe−N angles of bis(imino)pyridyl ligand) of triplet and especially quintet species differ significantly from singlet ones. Consequently, d_{z^2} and more significantly $d_{x^2-y^2}$ orbitals substantially relax upon occupation and subsequent geometrical changes.

We are fully aware of the fact that our approximate level of description of the system (B3LYP density functional in the Kohn−Sham formulation) is not ideal. Nevertheless, we believe that our calculations represent the best possible compromise between the description of two important aspects of the electronic structure of our species. The first issue is the description of dynamic correlation, which is generally believed to be decisively important for complexes of first-row transition metals. As a quite relevant example, we address the reader to the recent CASSCF/MRMP2/CASPT2 calculations of Hirao et al. on Fe(II) porphyrins,[7y,aa] in which a sharp contrast between CASSCF and MRMP2/CASPT2 results is described. The density functional method is expected to take care of dynamic correlation. The second aspect is nondynamic correlation, which density functional theory in the Kohn−Sham formulation is definitely unable to address. The results of Hirao et al.[7y,aa] reveal that most states of Fe(II) porphyrins are significantly multiconfigurational. In other words, the closed shell singlet calculations most likely represent an excited singlet state of the system, with a possibility of the

Downloaded by CARLI CONSORTIUM on June 29, 2009
Published on April 3, 2001 on http://pubs.acs.org | doi: 10.1021/om010126k

existence of much lower open shell singlet states. Moreover, the description of quintet and especially triplet states may also be defective due to a single-determinant description of the density. For example, Kozlowski et al. recently applied the same B3LYP methodology to various states of Fe(II) porphyrins.[7z] Comparison of the results of Kozlowski and co-workers with those of Hirao et al. reveals substantial differences (for example, the spin multiplicity of the ground state is different). Nevertheless, at a certain qualitative level, the results are comparable. The subsequent paper of Kozlowski et al. on the vibrational modes of Fe(II) porphyrin[7bb] suggests that agreement of the B3LYP results with certain experimental data may actually be indicative of appropriateness of the B3LYP description. In any case, the completeness of the description of the above-mentioned Fe(II) porphyrin system (calculation of vibrational modes) by the DFT method is yet to be matched by the multiconfigurational perturbative approach. The KS-DFT approach, which is biased toward a description of dynamic correlation, neglecting the nondynamic correlation, is still much more practical for systems as large as ours than the multireference perturbative approach. The meaning of such single-determinant calculations remains questionable. We can only hope that future, more sophisticated studies will prove that our level of approximation does not introduce severe errors in the overall picture of the chemical problem.

Concluding, among the three potential energy surfaces, the triplet and quintet are lower in the propagation region of the PES, but are significantly higher in the BHT region of the PES. We explain this result by the fact that the necessity of placing two ligands in the axial positions in the BHT-related species makes neither of the "d_σ" orbitals suitable for occupation by one (triplet) or two (quintet) electrons. In singlet species, the crystal field of the trichelating bis(imino)pyridyl ligand is not sufficient to compensate the excessive pairing of Fe's d electrons, and there is a need for a strong crystal field. The *anisotropy* created by the same trichelating bis(imino)pyridyl ligand, which destabilizes the equatorial position ($d_{x^2-y^2}$ orbital), determines the *z* axis domain (d_{z^2} orbital) to be a *very attractive place for electron density of ligands*. Consequently, the BHT-related configuration with two axial ligands is electronically very favorable. In contrast, in triplet and quintet species, the *z* axis domain is electronically saturated by *Fe's own electrons* (singly occupied d_{z^2} orbital). Moreover, a weaker crystal field is required, since the d electrons are less paired. Therefore, axial arrangement of ligands, in particular those of σ character (alkyl), is no longer necessary and becomes unfavorable. As a result, the BHT pathway on the singlet PES is energetically much lower than on higher spin states and, as our calculations suggest, is even comparable to chain propagation.

C. High Steric Bulk (HSB) System. The geometrical parameters of the IMOMM(B3LYP/BSII:MM3)-optimized structures of the HSB species are given in Supporting Information Table S6 (propagation-related species) and Table S7 (BHT-related species); energies of HSB species at the IMOMM(B3LYP/BSIII:MM3)// IMOMM(B3LYP/BSII:MM3) level, which are used in the text, are given in Table 2. The potential energy profiles

Table 2. Relative Energies ΔE^{IMOMM} and Energy Components, $\Delta\delta E^{MO}$ and ΔE^{MM}, of HSB Species *r*-I to *r*-VII at the IMOMM(B3LYP/BSIII:MM3)// IMOMM(B3LYP/BSII:MM3) Level Relative to *r*-I-*ax*-β + C_2H_4, in kcal/mol[a]

		ΔE^{IMOMM}			$\Delta\delta E^{MO}$			ΔE^{MM}		
process stage	specific isomer	singlet	triplet	quintet[b]	singlet	triplet	quintet[b]	singlet	triplet	quintet[b]
alkyl complex (*starting point*	(**I-*ax*-β**) + C_2H_4	0.0	−6.2	*b*	0.0	−2.7	*b*	0.0	0.6	*b*
of the chain propagation cycle)	(**I-*ax*-α**) +C_2H_4	11.3	*b*	*b*	3.1	*c*	*b*	1.4	*c*	*b*
	(**I-*eq*-α**) +C_2H_4	21.8	−15.3	−16.9	−3.4	−2.0	−1.0	−0.8	−0.7	−1.7
	(**I-*eq*-β**) +C_2H_4	16.6	−16.2	−16.9	2.6	−0.7	2.3	3.6	−2.6	−2.7
alkyl ethylene π-complex	(**II-*ax*′**)	−5.4 (5.4)	−16.4 (10.2)	*c*	2.6 (−2.6)	−1.7 (−1.0)	*c*	3.1 (−3.1)	0.1 (0.5)	*c*
(*immediate precursors for*	(**II-*ax*-β**)	2.3 (−2.3)	*c*	*b*	3.7 (−3.7)	*c*	*b*	17.9 (−17.9)	*c*	*b*
both insertion (chain propagation)	(**II-*ax*-α**)	6.3 (5.0)	*c*	*b*	7.8 (−4.7)	*c*	*b*	6.1 (−4.7)	*c*	*b*
and BHT chain termination)	(**II-*eq*-α**)	−2.8 (24.6)	−20.2 (4.9)	−21.9 (5.0)	1.7 (−5.1)	−0.1 (−1.9)	3.2 (−4.2)	3.1 (−3.9)	1.4 (−2.1)	0.6 (−2.3)
	(**II-*eq*-β**)	3.2 (13.4)	−17.3 (1.1)	−17.9 (1.0)	12.2 (−9.6)	2.3 (−3.0)	5.8 (−3.5)	6.1 (−2.5)	1.3 (−3.9)	2.5 (−5.2)
insertion (chain propagation) TS	(**III-**α)	−1.4 (1.4)	−8.9 (11.3)	−4.2 (17.7)	0.7 (−1.0)	−1.4 (−1.3)	1.5 (−1.7)	2.4 (−0.7)	−2.0 (−3.4)	0.5 (−0.1)
	(**III-**β)	5.2 (2.0)	*c*	*c*	7.0 (−5.2)	*c*	*c*	4.3 (−1.8)	*c*	*c*
alkyl complex (*ending point of the*	(**IV-*ax*-δ**)	−17.4	−23.1	*b*	1.1	1.2	*b*	2.9	1.9	*b*
chain propagation cycle)	(**IV-*ax*-γ**)	−17.3	−22.1	*b*	2.8	0.7	*b*	0.0	0.5	*b*
	(**IV-*ax*-β**)	−18.4	−29.8	*b*	1.5	−2.0	*b*	−1.1	−0.8	*b*
	(**IV-*eq*-β**)	*d*	*d*	−37.5	*d*	*d*	−1.9	*d*	*d*	−0.7
BHT chain termination TS	(**V**)	11.7 (9.4)	8.7 (28.9)	*d*	5.4 (1.7)	−10.4 (−10.3)	*c*	18.1 (0.2)	8.8 (7.4)	*d*
ethyl alkene π-complex	(**VI**)	3.1 (−4.1)	2.4 (−3.7)	*d*	7.7 (−8.4)	*e*	*d*	16.5 (−15.5)	6.4 (−4.5)	*d*
ethyl complex	(**VII**) +C_3H_6	−1.0	−1.3	*d*	−0.7	3.5	*d*	1.0	1.9	*d*

[a] For a definition of $\Delta\delta E^{MO}$ and ΔE^{MM}, see eq 4. In parentheses C_2H_4/C_3H_6 binding energy for species **II** and **VI** and C_2H_4 insertion and β-hydride transfer activation energies for species **III** and **V**, respectively. [b] Quintet species, although not distinguished by axial/equatorial classification, are listed as equatorial. [c] Unable to locate the stationary point. [d] Location of the stationary point not attempted. [e] The corresponding LSB stationary point does not exist.

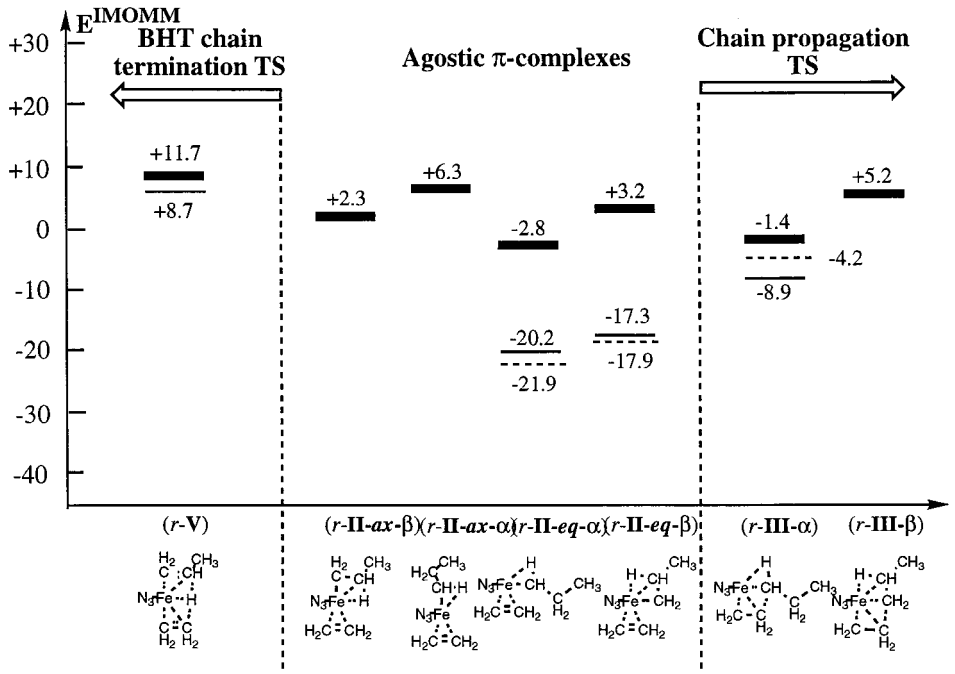

Figure 3. Competition between chain propagation and BHT chain termination mechanism in the HSB system. IMOMM-(B3LYP/BSIII:MM3)//IMOMM(B3LYP/BSII:MM3) potential energy surfaces (in kcal/mol) for alkyl ethylene π-complexes *r*-**II**, propagation transition states *r*-**III**, and BHT transition states *r*-**V**. Relative to *r*-**I-*ax*-β S** + C_2H_4. Singlet species: thick line; triplet species: thin line; quintet species: dashed line.

Downloaded by CARLI CONSORTIUM on June 29, 2009
Published on April 3, 2001 on http://pubs.acs.org | doi: 10.1021/om010126k

of the most important region of the potential energy surfaces are given in Figure 3. In section III.C, we describe only differences introduced by inclusion of the bulky ligands; our rationalization of these differences is given in the Rationalization subsection of Section III.C.

Alkyl Complexes. The HSB singlet alkyl complexes *r*-I **S** show the same trend as their LSB analogues; axial species are more stable than equatorial by 10−17 kcal/mol. As follows from comparison of Tables 1 and 2, inclusion of steric effects stabilizes species *r*-I-***eq***-α **S** and destabilizes species *r*-**I-*ax***-α **S** and *r*-**I-*eq***-β **S**, relative to *r*-**I-*ax***-β **S**. Introduction of the bulky substituents also increases the preference for equatorial species for the triplet; species *r*-**I-*eq***-α **T** and *r*-**I-*eq***-β **T** are more stable than axial *r*-**I-*ax***-β **T** by 9.1 and 10.0 kcal/mol, respectively. Results of constrained optimizations for the HSB system with fixed values of the N_y-Fe-C_p angle (see Supporting Information Table S8) resemble those for the LSB system. The axial → equatorial isomerization should have an extremely low barrier starting from *r*-**I-*ax***-β **T**, which is a very shallow minimum of the HSB potential energy surface. The quintet species *r*-**I Q** are the most stable among alkyl complexes (relative energy of −16.9 kcal/mol for both α- and β-isomers).

Monomer Capture. The ethylene binding energies for singlet alkyl π-complexes *r*-**II S** are −2.3 and 5.0 kcal/mol for axial species *r*-**II-*ax***-β **S** and *r*-**II-*ax***-α **S** and 24.6 and 13.4 kcal/mol for equatorial species *r*-**II-*ax***-α **S** and *r*-**II-*eq***-β **S**, respectively. Such a large difference in binding energies between the two groups of isomers results in approximately equal relative energies of axial and equatorial species *r*-**II S** (see Table 2). Nevertheless, the most stable isomer of singlet alkyl π-complexes for the HSB system is species *r*-**II-*ax*′ S** (with ethylene binding energy of 5.4 kcal/mol). The approach of ethylene at the equatorial position is the least sterically hindered one. We suggest that species *r*-**II-*ax*′ S** plays a role of nonreactive "sink" on the singlet surface.

We located only two equatorial isomers of alkyl π-complexes on the HSB triplet PES. Any attempt to minimize axial isomers converged to structures with either ethylene or alkyl ligands displaced to equatorial position. Strong electronic destabilization of axial positions in triplet species discussed in section III.B, combined with the steric hindrance of the axial positions to be explained in the Rationalization subsection, results in disappearance of the axial stationary points on the HSB PES for species *r*-**II T**. The ethylene binding energies in *r*-**II-*eq***-α **T** and *r*-**II-*eq***-β **T** are relatively small, 4.9 and 1.1 kcal/mol, respectively. The ethylene fragment in species *r*-**II-*ax*′ T** is bound by 10.2 kcal/mol. We do not expect these species to play any important role because of the high instability of the precursor alkyl complex *r*-**I-*ax***-β **T** with respect to isomerization to equatorial isomers. The ethylene binding energies for quintet HSB alkyl π-complexes are 5.0 kcal/mol for *r*-**I**-α **Q** and 1.0 kcal/mol for *r*-**I**-β **Q**. Again, the quintet is the lowest spin state for alkyl π-complexes.

The significantly decreased (in one case, even negative) ethylene binding energies for the singlet species discussed above suggest that ethylene approach to species *r*-**I S** is sterically hindered, and there may exist a sterically determined barrier for the formation of complexes *r*-**II S**. Nevertheless, as seen from Table 2, the singlet is an excited state for the HSB system, and therefore we did not address this minor issue of steric monomer coordination barriers in this paper.

There are two reasons to expect that the importance of steric hindrance for triplet and quintet species should be much smaller. First, it is likely that the triplet

Downloaded by CARLI CONSORTIUM on June 29, 2009
Published on April 3, 2001 on http://pubs.acs.org | doi: 10.1021/om010126k

precursors for monomer capture are the much more stable equatorial rather than axial species. In the quintet alkyl complexes *r*-**I Q**, as well as in the triplet equatorial species *r*-**I-*eq* T**, the N_y-Fe-C_p' angle is significantly larger than 90°. Consequently, the two axial positions are not hindered, neither by the alkyl ligand itself nor by an agostic C−H bond (see section III.B). This contrasts with the case of singlet complexes *r*-**I S**, in which the empty d_{z^2} orbital interacts extremely favorably with either the σ-donating negatively charged carbon of the alkyl ligand or the agostic C−H bond. The second reason for smaller steric hindrance of ethylene approach to quintet and equatorial triplet alkyl complexes is also related to the fact that the d_{z^2} orbital is always singly occupied in these species. As a result, the Fe−ethylene interaction is much weaker, the $Fe-C_e'$ and $Fe-C_e''$ distances are larger, and the resulting steric destabilization of the bulky substituents by the ethylene fragment is smaller.

Furthermore, although a small ethylene coordination barrier may exist on both triplet and quintet surfaces (which are the two lowest states in our HSB system), it should have little effect on the main mechanistic topic of this paper, the question of competition between chain propagation and BHT chain termination. As will be seen, the BHT chain termination and chain propagation processes, in the case of the HSB system, have the *same* precursor, alkyl π-complex *r*-**II-*eq*-α T**. Any barrier existing prior to that point of the catalytic propagation cycle, including a monomer uptake barrier, may change the absolute effective rate of the two processes, but should not influence their relative rate.

Certain geometrical changes upon introduction of bulky ligands are observed in singlet and triplet equatorial alkyl π-complexes, as well as, to a smaller extent, in both quintet alkyl π-complexes. Namely, the $Fe-C_e'$ and $Fe-C_e''$ bonds are elongated, by up to 0.1 Å in singlet and 0.3−0.5 Å in much more flexible triplet and quintet species. Notably, β-isomers are deformed more significantly (see Tables S1 and S5).

Ethylene Insertion. Chain propagation barriers on the HSB singlet surface are extremely small, 1.4 kcal/mol for TS *r*-**III-α S** and 2.0 kcal/mol for *r*-**III-β S**. We were able to locate only one insertion TS, *r*-**III-α**, on both triplet and quintet PES. The insertion barriers, although decreased compared to the LSB case, are still relatively high, 11.3 kcal/mol for triplet and 17.7 kcal/mol for quintet. As seen from Table 2, the energetically lowest insertion TS is located on the triplet surface. However, as discussed in section III.A and III.B, we can expect the quintet surface to come close to the triplet after inclusion of the Gibbs free energy correction due to weaker Fe−ligand interactions in the quintet species. We did not calculate an entropy correction, as frequency calculations are not implemented in the IMOMM program.

Alkyl Complexes. The insertion products for all three spin states are geometrically and energetically very similar to these for the LSB system. The most stable isomer is *r*-**IV-β Q**, with a relative energy of −37.5 kcal/mol; the most stable singlet (*r*-**IV-*ax*-β S**) and triplet (*r*-**IV-*ax*-β T**) species are, respectively, 19.1 and 7.8 kcal/mol higher. However, we expect triplet equatorial species *r*-**IV-*eq* T** to be comparable in energy to quintet species.

BHT Chain Termination. We excluded quintet species from consideration of BHT, since the quintet TS is energetically the highest one in the case of the LSB system. The precursor for BHT chain termination on the singlet surface is species *r*-**II-*ax*-β S**; as discussed above, this species is highly destabilized by inclusion of bulky substituents, but still exists as a local minimum on the singlet PES. In contrast, axial triplet species *r*-**II-*ax*-β T** no longer exists for the HSB system due to steric destabilization. Analogously to the quintet species in the LSB case, the α-configuration of equatorial triplet alkyl complexes, species *r*-**II-*eq*-α T** in the case of the HSB system is the most suitable precursor for BHT chain termination.

The singlet BHT transition state *r*-**V S** lies energetically very high (relative energy of +11.7 kcal/mol). In fact, it is higher than the triplet TS *r*-**V T** (relative energy of +8.7 kcal/mol). The triplet TS is largely asymmetrically displaced from the geometry of the LSB system; the N_y-Fe-C_p' and N_y-Fe-C_e' angles are 90.5° and 102.3° compared to approximately equal values of 103.7° and 101.8° in case of the LSB system.

Concluding, in case of the high steric bulk system, BHT (with relative energy of +8.7 kcal/mol for the energetically lowest TS *r*-**V T**) cannot compete with chain propagation (with relative energy of the lowest energy TS being −8.9 kcal/mol).

Summary: "High Bulk System" Catalysts. The most significant result of introduction of bulky substituents is the enormous destabilization of the entire singlet PES. Triplet and quintet species are also destabilized, but to a smaller degree. Due to perpendicular orientation of the aryl rings relative to the plane of the pyridyl ligand, the bulky substituents in ortho positions selectively destabilize axial positions. Consequently, species in which these axial positions are occupied (structures with axial alkyl, π-complexes with axial alkene, and compounds with strong agostic interaction via axial positions) are destabilized more than others. As was explained in section III.B, singlet axial compounds are always preferred, for electronic reasons, over equatorial, while the situation for the triplet surface is reversed. Moreover, since the singlet species require stronger ligand field, the agostic interaction via axial positions (which is possible only in equatorial species) is strong, which leads to steric destabilization of equatorial species upon introduction of bulky ligands. Similarly, agostic and alkene binding by axial position in equatorial singlet species is much stronger than in triplet and quintet analogues. Effectively, both axial and equatorial singlet species are significantly destabilized, and the entire singlet PES is shifted up relative to triplet and quintet.

The chain propagation barriers on the HSB singlet PES are quite low, 1.4 and 2.0 kcal/mol. While the HSB BHT barrier, 9.4 kcal/mol, is comparable to that for the LSB system, the entire BHT region of the singlet PES is significantly destabilized by the bulky substituents. The singlet BHT TS lies 13.1 and 6.5 kcal/mol *higher* in energy than the two singlet propagation transition states. The Curtin−Hammett principle suggests that, provided the axial → equatorial conversion is fast, chain

Downloaded by CARLI CONSORTIUM on June 29, 2009
Published on April 3, 2001 on http://pubs.acs.org | doi: 10.1021/om010126k

propagation is preferred over BHT chain termination on the singlet surface.

For the HSB system, the singlet becomes an excited state for studied regions of the PES. The profiles for the two low lying states, triplet and quintet, are closely comparable. The triplet chain propagation and BHT chain termination barriers are 17.7 and 26.0 kcal/mol. We did not attempt to locate the quintet BHT TS, and the triplet BHT TS lies 17.6 and 12.9 kcal/mol higher than the triplet and quintet propagation TS′ correspondingly.

While the triplet chain propagation TS is the lowest in energy, inclusion of the Gibbs free energy correction would most likely make the quintet and triplet closely comparable. Therefore, either of the two states is suitable for propagation. The BHT chain termination pathway is highly destabilized by the bulky substituents, in qualitative agreement with experimental observations. Nevertheless, we cannot speculate on the overall balance between propagation and termination, since we do not study the other chain termination mechanism experimentally confirmed to be dominant for high steric bulk species, transmetalation (chain transfer to counterion).

Within the scope of the present paper, the main mechanistic result of destabilization of the axial positions is that the BHT chain termination mechanism is no longer competitive with chain propagation. Figure 3 summarizes the potential energy profiles for competition between BHT and chain propagation for the HSB system. The lowest energy BHT TS, triplet species *r*-**V T**, is 17.6 kcal/mol higher than the energetically lowest propagation TS (*r*-**III-**α **T**). One may expect that upon inclusion of the Gibbs free energy correction, quintet propagation TS *r*-**III-**α **Q** would become close to the triplet analogue. Another important mechanistic result of inclusion of steric effects is a decrease in chain propagation barrier, apparently due to greater destabilization of the precursor complexes *r*-**II-*eq*** than that of transition states *r*-**III**. The ethylene fragment in alkyl π-complexes *r*-**II-*eq*** is displaced farther from the Fe center, which leads to decrease in both the ethylene binding energy and the insertion barrier.

Concluding, our description of the high steric bulk system may be summarized as follows. Throughout many steps of the entire catalytic cycle, the system stays on either the triplet or quintet state, never visiting the singlet. The chances for a BHT step to take place are marginal and should be smaller than that of the other proposed chain termination mechanism, transmetalation. This picture is consistent with the experimentally observed suppression of BHT upon increase in the steric bulk.

Rationalization of Steric Effects. In the IMOMM method, the total energy of the "real" system at the geometry R^{IMOMM} optimized at this IMOMM level can be expressed as[15]

$$E^{IMOMM} = E^{MO} + E^{MM} \quad (1)$$

On the other hand, take the corresponding "model" system (the part which is handled by the MO method in the IMOMM method) at the geometry ${R_0}^{MO}$ optimized with the pure MO method (at the same level used in the IMOMM method) and call its energy ${E_0}^{MO}$. Using this, the IMOMM energy in eq 1 can be rewritten as

$$E^{IMOMM} = {E_0}^{MO} + \delta E^{MO} + E^{MM} \quad (2)$$

where

$$\delta E^{MO} = E^{MO} - {E_0}^{MO} \quad (3)$$

From eq 2, the energy of the IMOMM species relative to a reference species (in the present work, the singlet state of *r*-**I-*ax*-**β + C_2H_4) can be written as

$$\Delta E^{IMOMM} = \Delta {E_0}^{MO} + \Delta\delta E^{MO} + \Delta E^{MM} \quad (4)$$

Since our model system in the IMOMM calculation is nothing but the model system discussed for the LSB case above, the first term in eq 4, $\Delta {E_0}^{MO}$, is the relative energy of *the LSB species* shown in Table 1. The second term, $\Delta\delta E^{MO}$, represents the relative change of the model MO energy due to its distortion from its original stationary point ${R_0}^{MO}$ due to the presence of the bulky ligands (MM part) and may be called relative *steric distortion* energy. The steric distortion energy and the associated change in the MO part of the geometry in R^{IMOMM} from ${R_0}^{MO}$ allow for assessment of the magnitude of the effects of a bulky group on the energy and geometry of the MO part.[29] The third term, ΔE^{MM}, represents the relative *steric potential* energy of the MM part at the IMOMM-optimized geometry. $\Delta\delta E^{MO}$ and ΔE^{MM}, as well as ΔE^{IMOMM}, are shown in Table 2. One should note that, although $\Delta\delta E^{MO}$ is listed in Table 2, there exists a substantial value of steric distortion energy δE^{MO} = 5.0 kcal/mol already for the reference species (*r*-**I-*ax*-**β + C_2H_4). We will base our following analysis on $\Delta\delta E^{MO}$ and ΔE^{MM} values in Table 2.

The major impact of bulky ligands on the catalytic (Fe) center is destabilization of the axial positions due to interaction of the axial ligands with the H atoms of ^{i}Pr groups. This is the dominant factor, which explains most of the observed effects. In particular, we make the following observations.

1. Species with two axial ligands are destabilized more than those with one axial ligand.

2. For axial species, β-species are the least destabilized; steric effects are more pronounced for α-, δ-, and γ-configurations. In contrast, among equatorial species, α-isomers are destabilized less than the β-analogues.

3. In triplet species, the impact of bulky substituents on a propyl ligand are more significant than that on an ethyl ligand. At the same time, the difference between ethylene and propylene is much smaller. The alkene ligands, of which the π-binding is weakened by a single electron on the d_{z^2} orbital to a greater degree than σ-binding of the alkyl ligands, are consequently much

(29) The basis set used for geometry optimization of the electronically important part of the HSB system is different from that used for optimization of the geometry of the LSB species. Namely, the bis-(imino)pyridyl ligand is treated with the D95V basis set in the HSB system and with the 3-21G basis set in the HSB system; the FeC_5H_{11} subsystem is treated with the D95V basis set in both BSI and BSII. To assess the difference in geometrical parameters introduced by the variation in the basis set, we reoptimized all nine LSB species *m*-**I** at the B3LYP/BSII level and performed B3LYP/BSIII single-point calculations. Supporting Information Table S9 gives the absolute energies at the two levels, B3LYP/BSIII//B3LYP/BSI and B3LYP/BSIII//B3LYP/BSI, as well as the value of difference between the two. The range of the difference is −2 to +2 kcal/mol.

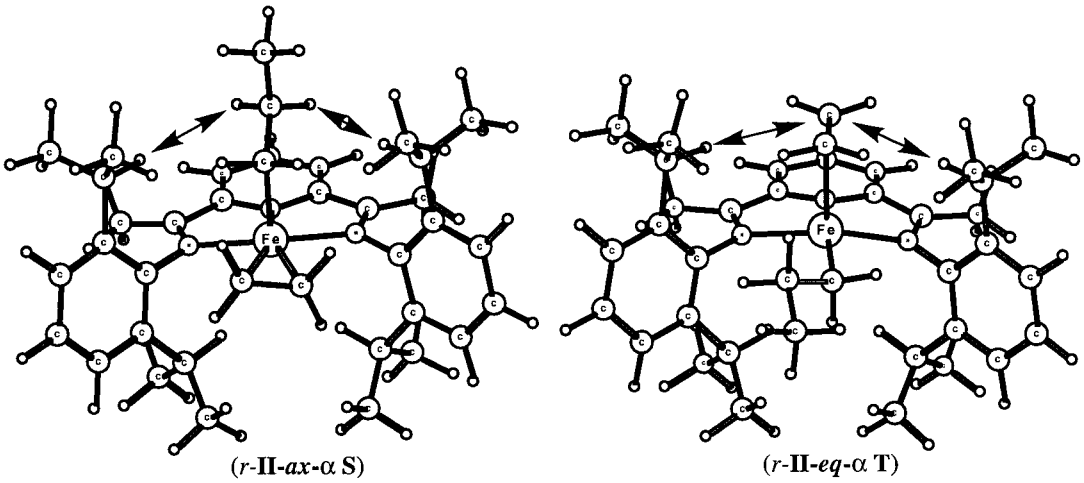

Figure 4. Structure of the most stable singlet, *r*-**II-*ax*-α S**, and triplet, *r*-**II-*eq*-α T**, HSB alkyl ethylene π-complexes. The arrows illustrate the most dominant repulsive steric interactions of the bulky ortho substituents of the Ar rings with axial ligands.

Downloaded by CARLI CONSORTIUM on June 29, 2009
Published on April 3, 2001 on http://pubs.acs.org | doi: 10.1021/om010126k

easier to displace farther from the Fe center than alkyl ligands. As a result, due to higher *steric distortion* of the MO part of the reactants compared to that of the products, the transition state for the (propyl + ethylene) → (propene + ethyl) transformation on the triplet HSB PES, *r*-**V T**, becomes *electronically* an early TS. Such effects are not found for singlet species, in which the d_{z^2} orbital is unoccupied, and π-binding of alkene ligands remains strong.

4. *Steric distortion* of alkyl ethylene π-complexes *r*-**II-*eq*** is larger than that of insertion transition states *r*-**III**, which results in decreased ethylene insertion barriers.

5. Quintet species, for which the N_y-Fe-C_p angle is smaller than in triplet isomers due to the $d_{x^2-y^2}$ orbital being singly occupied,[30] are destabilized more than triplet analogues.

6. Increase of the steric bulk on one side of the bis(imino)pyridyl−Fe plane directly influences ligands on the other side. For example, β-conformation of the alkyl ligand is unfavorable in equatorial π-complexes, in which the other axial position is occupied by the ethylene fragment. In another example, quintet π-complexes, in which the alkyl chain is displaced from the equatorial position toward the vacant axial position compared to equatorial triplet π-complexes (see Table S6), are sterically destabilized stronger than the latter. A recent experimental paper[1e] indicates that substitution of the Me groups on the imino carbon atoms with hydrogens decreases the average length of the produced polymers. We suggest that Me groups, which interfere with relaxation of the ortho substituents outside axial positions, amplify this effect of steric coupling of the two trans axial positions.

Figure 4 illustrates the destabilization of the axial positions by the "bulky" ortho substituents of the Ar rings. For the singlet alkyl ethylene π-complexes, in which electronic effects favor the axial position for the alkyl ligand, the preferred mode of ethylene coordination is by the equatorial position. The steric hindrance of the equatorial position is much smaller compared to that for the second axial position. At the same time, since the d_{z^2} orbital is singly occupied in triplet alkyl ethylene π-complexes, the alkyl itself occupies the equatorial position. Correspondingly, the bulkier the ligands in the axial positions, the larger the steric destabilization.

As was noted in the conclusion of section III.B, the presence of the trichelating bis(imino)pyridyl ligand in the coordination sphere of Fe results in a *deficiency in the electron density* in the *z* axis domain of the Fe center in singlet species. There are two ways of saturating this deficiency. The first is saturation with *ligands' electrons* by the axial arrangement of ligands (alkyl, alkene, agostic C−H) in singlet compounds. The second way is population of the d_{z^2} orbital by *Fe's own* electrons, which is associated with an *increase in the value of total spin* and is realized in triplet and quintet species. Clearly, the *steric hindrance* (imposed by the ortho substituents of the Ar rings) associated with the first way is much more severe than that of the second. Consequently, the entire singlet PES is shifted up in energy, especially in the BHT region.

IV. Comparison with the Results of Deng et al.

Recently, Deng et al.[5a] applied IMOMM(BP86:Amber) methodology to chain propagation and BHT chain termination processes catalyzed by the same low and high steric bulk systems. In this section, we compare our results with those of Deng et al., emphasizing the important qualitative differences and suggesting possible interpretations.

1. The BP86 density functional employed by Deng et al. disfavors high-spin states compared to B3LYP used by us. For example, the relative energies of species **2C(t)** and **2C** in the paper of Deng et al.[5a] are −2.7 and −6.2 kcal/mol, respectively, while the values for corresponding species in our study, *r*-**II-*eq*-β T** and *r*-**II-*eq*-β S**, are −17.3 and +3.2 kcal/mol, respectively. The magnitude of difference between B3LYP and BP86 singlet−triplet separations varies from species to species, with the general trend being clear: B3LYP favors triplet, BP86 prefers singlet. Furthermore, using the B3LYP density functional, we found the quintet state

(30) Describing the quintet species as distorted from octahedral (square pyramid) geometry, we avoid complications of switching to trigonal bipyramid point of view at the ligand arrangement, keeping the effect of the bulky ligands (hindrance of the axial positions of the octahedral configuration) clearer.

Downloaded by CARLI CONSORTIUM on June 29, 2009
Published on April 3, 2001 on http://pubs.acs.org | doi: 10.1021/om010126k

lying low in energy (comparable to triplet), while Deng et al. suggest that the BP86-produced quintet is too high to play any role in the catalytic cycle. Since Deng et al. do not give any results on the model ("generic") triplet species, the comparison of singlet−triplet separation is possible only for the full system. Although in the latter case, the difference between the calculation procedure of Deng et al. and that used by us is additionally influenced by the choice of molecular mechanics force field (Deng et al. use Amber and we use MM3(92)), we suggest that the main component of that difference is due to the density functional. Our suggestion is supported by a recent paper[18s] on a closely related Co(II) catalytic system, in which Margl et al. directly compared B3LYP and BP86 for doublet and quartet states of several species (see Supporting Information of ref 18s). The observed analogous trend (the high-spin state is much more stable with B3LYP compared to BP86) has been quite reasonably explained by the presence of an "exact" Hartree−Fock exchange component in the B3 exchange functional. Although we are unable to track the origin of the assumption of Margl et al.[18s] that B3LYP results represent a lower bound for the high-spin/low-spin energy difference, we agree that this difference would definitely decrease upon mixing the HF "exact" exchange into the exchange density functional, when going from the B to B3 exchange functional. The latter trend is in line with the observed differences between the results of Deng et al. and those in the present paper.

A benchmarking "calibration"[31] of both B3LYP and BP86 functionals would have been one of the ways to solve the arising controversy. The main objective of such a calibration must be the performance of the two density functionals for the purposes of evaluation of the energy separation between electronic states of different total spin for highly coordinated Fe(II) complexes (or, more generally, complexes of first-row transition metals). Such a benchmark study should compare the results produced by the two calculations either with results of high-level ab initio calculations or with experimentally derived data. On the basis of the literature search performed, we conclude that little is currently conclusively known about the subject of the present controversy, the energy separation between PESs of different spin states. To the best of our knowledge, this aspect of the performance of the two functionals has not been systematically compared in the literature. We emphasize that a benchmark relevant to the present chemical problem should necessarily address a highly coordinated system. Both experiment and high-level ab initio calculations on spin state separations in small, coordinatively unsaturated Fe-containing species have been related to the results produced by both BP86 and B3LYP functionals.[32] The extent of such benchmarks is extremely limited. More importantly, it is doubtful that the results on small ions and molecules should be taken into account considering the substantially larger number of ligands in the Fe(II) species in the present study. The established[31] problem of the s^0d^n vs s^1d^{n-1} description by DFT methods dominates the picture for coordinatively unsaturated molecules, but should not play any role for systems like ours. On the other hand, there is little data on spin state separation in larger molecules, and a benchmark may be inconclusive.[32a]

We performed calculations on a model for the precursor dichloride complex (see Tables S10, S11 and Figure S1) with both B3LYP and BP86 functionals. The ground state for both functionals is the quintet. Nevertheless, while for B3LYP the triplet minimum lies 13.3 [16.0] kcal/mol higher in energy [in brackets, Gibbs free energy], the BP86 separation is much smaller, 0.0 [3.0] kcal/mol. We argue that the energy separation produced by BP86 is too small provided the experimentally established quintet ground state for the precursor.[1b,c] A recent study[33] provides additional support for accuracy of the B3LYP functional. Any further speculations on appropriateness of either functional for the system under study must rely on rigorous benchmarks, which is beyond the scope of the present paper.

2. The destabilization of axial triplet species relative to equatorial isomers due to a singly occupied d_{z^2} orbital is smaller in the results reported by Deng et al. than that observed by us. We explain this fact with the same reasoning: the difference in the two functionals used in the description, particularly of the interaction of a singly occupied d_{z^2} orbital with the alkyl ligating orbital. Indeed, the difference between relative energies of singlet species **1C** and **1A**, which includes both the trans influence of the pyridyl nitrogen and the (insignificant for alkyl complexes) steric effects, is 15.9 kcal/mol, which is close to our difference between *r*-**I-*ax*-*β* S** and *r*-**I-*eq*-*β* S** of 16.6 kcal/mol. At the same time, according to BP86 calculations of Deng et al., the energies of **1C(t)** and **1A(t)** differ by +3.4 kcal/mol, while our B3LYP results give a value of −10.0 kcal/mol. Again, careful and thorough benchmarks are required in order to assess the performance (and its consistence) of either of the functionals for this type of system.

3. Combined, the two factors described above lead to an interesting difference in an important mechanistic aspect. Calculations of Deng et al. produce the singlet as the ground state even for the high steric bulk system. Due to trans influence of the pyridyl's ligating nitrogen, the axial species **1A** (*r*-**I-*ax*-*β* S** in our notation) is the most stable alkyl complex. As discussed by us in section III.C and by Deng et al., approach of ethylene to the axial position of *r*-**I-*ax*-*β* S** (**1A**), either frontside or backside, is highly hindered by the bulky substituents, which leads to the existence of monomer uptake barriers. Moreover, according to Deng et al., species *r*-**I-*ax*-*β* S** (**1A**) is the branching point between chain propagation and chain termination mechanisms on the ground singlet PES. They find steric bulk contributes to the barriers of both processes, but most importantly to that of BHT chain termination (frontside attack).

At the same time, our ground state for the HSB system is triplet, with quintet being very close. Furthermore, in contrast with the results of Deng et al.,

(31) (a) Koch, W.; Holthausen, M. C. *A Chemist's Guide to Density Functional Theory*; Wiley-VCH: Weinheim, FRG, 2000; pp 251−259. (b) Holthausen, M. C.; Fiedler, A.; Schwarz, H.; Koch, *W. J. Phys. Chem*. **1996**, *100*, 6236. (c) Holthausen, M. C.; Koch, W. *J. Am. Chem. Soc.* **1996**, *118*, 9932.

(32) (a) Wang, W.; Weitz, E. *J. Phys. Chem. A* **1997**, *101*, 2358. (b) Filatov, M.; Shaik, S. *J. Phys. Chem. A* **1998**, *102*, 3835.

(33) Chen, G.; Espinosa-Perez, G.; Zentella-Dehesa, A.; Silaghi-Dumitrescu, I.; Lara-Ochoa, F. (Tetrakis(2-pyridylmethyl)ethylenediamine)iron(II) Perchlorate. Study of Density Functional Methods. *Inorg. Chem*. **2000**, *39*, 3440.

Downloaded by CARLI CONSORTIUM on June 29, 2009
Published on April 3, 2001 on http://pubs.acs.org | doi: 10.1021/om010126k

our triplet equatorial species are more stable than axial isomers. The interaction of the Fe center with the ethylene fragment in triplet species is much weaker than in singlet species. Even if a barrier exists, it should be smaller than for the singlet ground state of Deng et al. Moreover, according to our mechanism, the branching between chain propagation and BHT chain termination on our low lying triplet and quintet PESs takes place past the monomer coordination. All that diminishes the importance of a monomer coordination barrier in our picture of the process.

It must be noted that the IMOMM methodology in the implementation currently used by us (and, supposedly, by Deng et al.) is unable to locate transition states for which the reaction coordinate has significant components along "steric" degrees of freedom, such as opening of the bulky substituents in the present HSB systems and alike. Energy is minimized along all "steric" degrees of freedom in "microiterations" of the present version of IMOMM.[15a] The Hessian (second derivative) matrix is assumed to be block-diagonal, with the "steric" block being positively defined.[34] Hence, location and meaning of a monomer coordination transition state is questionable with the IMOMM methodology of Maseras et al. More appropriate would be an optimization using the full gradient and Hessian matrix as adopted in recent implementation of the ONIOM method[35] and a dynamic approach such as recently applied by Woo et al.[18y] to a similarly sterically complicated Ni(II) diimine olefin polymerization catalysts.

4. Further differences (supposedly determined by the choice of density functional) of lesser importance exist between our results and results of Deng et al. As discussed by Musaev et al.,[3c] the strength of metal−ligand interactions is higher with the BP86 than with the B3LYP method. This leads to stronger Fe−C_2H_4 interactions in studies of Deng et al., thus emphasizing the role of steric barriers in the case of HSB systems.

5. Another difference is the absence of an equatorial approach of ethylene in the picture of Deng et al. According to our results, stationary point *r*-**II-*ax′* S** *is the most stable among all HSB alkyl π-complexes*. The equatorial approach of the monomer is less hindered sterically and may seriously question the appropriateness of the singlet PES for propagation in the case of HSB systems (see Figure 4). In contrast, the most stable triplet alkyl complexes, according to our results, are those with the equatorial position occupied by the alkyl ligand.

V. Conclusions

On the basis of our B3LYP and IMOMM(B3LYP:MM3) results, we draw the following conclusions.

1. Intrinsically, triplet and quintet states are generally preferred over singlet for most of the low steric bulk (LSB) species under study. An exception is the BHT region of the PES, in which the singlet becomes the ground state. This exception, as well as the fact that the triplet PES prefers the equatorial position for the alkyl ligand over axial, is determined by the destabilization imposed by the ligand environment onto the two "d_σ" orbitals, most importantly, the d_{z^2} orbital.

2. Extension of the basis set from DZ to TZP stabilizes higher spin states, which indicates that DZ quality is not sufficient for description of energetics of the Fe(II) complexes in the problem.

3. Inclusion of the Gibbs free energy correction stabilizes higher spin states, in which the metal−ligand antibonding orbitals become populated. We explain this effect by the corresponding metal−ligand vibration modes becoming "floppier". As a consequence, the zero point energy and the entropy correction decrease with the increase of the spin value.

4. For the LSB system, relative Gibbs free energies of propagation transition state *m*-**III-α Q** and the only feasible BHT transition state *m*-**V S** are comparable, which makes *β*-hydride transfer a competitive chain termination mechanism. Effectively, relatively short oligomer chains with unsaturated end groups should be produced, in agreement with the experimentally observed formation of α-olefins by catalytic systems with a single ortho substituent.

5. Inclusion of two bulky ortho substituents on the Ar rings (our model of a high steric bulk (HSB) system) results in steric destabilization of the axial positions. Consequently, BHT on any state is no longer competitive with chain propagation, which takes place most likely on triplet and, possibly, on quintet PESs. We correlate this result with our interpretation of the experimental data: suppression of BHT as a chain termination mechanism with the increase of steric bulk.

6. The strong crystal field required for stabilization of singlet species (particularly, of the d_{z^2} orbital) is most favorably imposed by ligands in axial positions, ultimately by two strong ligands as in BHT-related species, but to some degree in all energetically low singlet species. On the other hand, the steric destabilization imposed by the ortho substituents on the axial positions is enormous. Consequently, the singlet is destabilized relative to triplet and quintet species, the latter being suited for chain propagation better than for BHT.

7. Presently, we cannot suggest a quantitative picture of the process for either low or high steric bulk extreme cases. For the low steric bulk system, a comparison between chain propagation and the dominant chain termination (BHT) pathways is precluded by the fact that the former takes place on a quintet (and possibly triplet) spin state, while the latter occurs on a singlet PES. For the high steric bulk system, according to experimental results, the prevailing chain termination mechanism is transmetalation, which we do not take into account. The present study provides a detailed description of the three potential energy surfaces. The assumption of rapid spin interconversion is able to explain two experimental observation: the competitiveness of BHT chain termination and chain propagation for low steric bulk systems and the suppression of the BHT pathway upon increase in steric bulk. We suggest that chain propagation takes place on triplet and quintet surfaces, which is the main new result of the present paper. Future studies are necessary to validate this result and to describe the overall propagation/termination balance by addressing the missing pieces of the picture, two of them being the spin interconversion rate

(34) Maseras, F. Private communication.
(35) Dapprich, S.; Komaromi, I.; Byun, K. S.; Morokuma, K.; Frisch, M. J. *J. Mol. Struct.: THEOCHEM* **1999**, *461−462*, 1.

and the mechanism of the transmetalation chain termination pathway.

Acknowledgment. The authors deeply thank Dr. Feliu Maseras, one of the authors of the IMOMM methodology, for helpful discussions and advice. The authors thank Dr. Karl S. Hagen and Dr. Joel M. Bowman for insightful comments. The present research is in part supported by a grant (CHE96-27775) from the National Science Foundation. Acknowledgment is made to the Cherry L. Emerson Center of Emory University for the use of its resources, which is in part supported by a National Science Foundation grant (CHEM-0079627) and an IBM Shared University Research Award. Computer time allocated at the Center for Supercomputing Applications (NCSA) and Maui High Performance Computer Center (MHPCC) is also acknowledged.

Supporting Information Available: Table S1. Selected structural parameters of all the studied species relevant to chain propagation process in "low steric bulk" (LSB) system. **Table S2**. Selected structural parameters of all the studied species relevant to β-hydride transfer (BHT) chain termination process in "low steric bulk" (LSB) system. **Table S3**. Total energies of LSB species, *m*−**I** to *m*−**VII**, at B3LYP/BSI//B3LYP/BSI and B3LYP/BSIII//B3LYP/BSI levels. **Table S4**. Values of ZPE and Gibbs free energy corrections for LSB species, *m*-**I** to *m*-**VII**, at B3LYP/BSI level. **Table S5**. Energies of LSB species *m*-**I T** with α- and β- relative orientation of propyl chain and Fe center optimized with fixed values of N_y-Fe-C_p angle. **Table S6**. Selected structural parameters of all the studied species relevant to chain propagation process in "high steric bulk" (HSB) system. **Table S7**. Selected structural parameters of all the studied species relevant to β-hydride transfer (BHT) chain termination process in "high steric bulk" (HSB) system. **Table S8**. Energies of "high steric bulk" species *r*-**I T** with α- and β- relative orientation of propyl chain and Fe center; optimized with fixed values of N_y-Fe-C_p angle. **Table S9**. Total B3LYP/BSIII energies of LSB alkyl complexes, *m*−**I**, optimized at B3LYP/BSI and B3LYP/BSII levels. **Table S10.** Comparison of B3LYP/BSIII//B3LYP/BSI and BP86/BSIII//BP86/BSI energies and Gibbs free energies for a model of the precursor dichloride complex, *m*-**0**. **Table S11.** Selected optimized geometrical parameters of the precursor dichloride complex, *m*-**0**, at B3LYP/BSI and BP86/BSI levels of theory. This material is available free of charge via the Internet at http://pubs.acs.org.

OM010126K

Downloaded by CARLI CONSORTIUM on June 29, 2009
Published on April 3, 2001 on http://pubs.acs.org | doi: 10.1021/om010126k